Principal Investigator
Brent Marquis, Director of Science and Technology
Sensor Research and Development Corporation
17 Godfrey Drive
Orono, ME 04473
bmarquis@srdcorp.com
(207) 866-0100 ext. 215

Institution Receiving Award
Sensor Research and Development Corporation
17 Godfrey Drive
Orono, ME 04473
(207) 866-0100

Project Title: "Mining Environment Detection System"
Date / Report Number: March 30, 2012 / Report 1 (Final Report)
Co-Investigators: None
Project Director / Sponsor: Linda Frederick / NIOSH
Grant Number: 1R43OH009563-01A1
Project Starting Date / Ending Date: September 1st, 2011 / February 29th, 2012
Date Final Report Completed: March 30, 2012

1. Table of Contents

2. List of Terms and Abbreviations

AMS - Atmospheric Monitoring System
COTS - Commerical off the Shelf
CWAs - Chemical Warfare Agents
FID - Flame Ionization Detector
GC - Gas Chromatography
IDLH - Immediately Dangerous to Life and Health
LDA - Linear Discriminant Analysis
LLOD - Lower Limit of Detection
MAC - Media Access Control
MEMS - Micro-Electromechanical System
MFC - Mass Flow Controller
MS - Mass Spectrometer
MSHA - Mine Safety and Health Administration
MTD - Maximum Transmission Distance
PELs - Permissible Exposure Levels
PFA - Probability of a False Alarm
RBF - Radial Basis Function
RH - Relative Humidity
RSD - Relative Standard Deviation
SMO - Semiconducting Metal Oxide
SRD - Sensor Research and Development Corporation
SVM - Support Vector Machine
TCD - Thermal Conductivity Detector
TICs - Toxic Industrial Chemicals
VHP - Verified High Purity
WMN - Wireless Mesh Network
WSN - Wireless Sensor Network

3. Abstract

In Phase I, SRD demonstrated the successful design and implementation of a solid-state sensor array, coupled with advanced algorithms, capable of autonomous operation and real-time, detection, identification, and quantification of four mining gases including methane (CH_4), carbon monoxide (CO), oxygen (O_2), and carbon dioxide (CO_2) within mining conditions. SRD exposed the sensor array to gas scenarios that simulated two mining conditions including sudden release of a mine gas via a gas pocket and gradual release of gas from fissures or from daily exposure. To focus on an early warning detector, gas testing focused on low, high and critical levels for each mining gas. SRD used the sensor array response data, obtained from all gas testing, to implement a hierarchical algorithm approach to first detect, then identify, and finally quantify each mine gas.

The Phase I performance metrics of the sensor array, coupled with algorithms, was determined including detection times (10-30 seconds), precision (76.7-97.5%), accuracy (87.8-97.7%), and Probability of False Alarms (0-5.5%). The Phase I sensor array and algorithms operated autonomously, without any calibration, while providing precise and accurate detection, identification, and quantification of each mine gas within seconds with no false alarms except for lower CO_2 levels. SRD also integrated and verified a gore water/particulate filter along with a custom flame arrestor to mitigate harsh, and potentially explosive, conditions within mines. SRD also evaluated and verified that a commercial off the shelf (COTS) 900 MHz wireless module demonstrated superior transmission range and was successfully implemented to form a 4-node mesh network that extends wireless transmission range. It is anticipated that a larger mesh network would relay sensor array data to a single base station from any point within a mine, allowing the mine to be chemically mapped and monitored for impending dangerous conditions.

In Phase I, SRD has established the necessary technical foundation to build upon in Phase II to focus on designing, constructing, verifying, and field-testing prototype mine detectors. The Phase I results demonstrate the sensor array, algorithm, and wireless mesh network, will dramatically improve occupational safety and health of mine workers by chemically mapping the entire mine to provide early warning of possible explosive conditions. The base station will receive early warning of impending threats and precise locations to allow mine workers to be directed through a safe evacuation route. SRD's mining detectors will be low-cost (~$500-$750) and small enough to wear or carry and be mounted in fixed locations or on machinery. Each detector will have integrated wireless transmission communications and support real-time, continuous self-diagnostics to extend operational lifetime. The simple power ON / power OFF detector operation will not require any calibration, saving mine workers time to focus on other safety gear.

In Phase II, SRD will construct, verify, and field test prototype mine detectors in two separate field test trials, within an active mine, for a spiral development to ensure the prototype mine detectors meet the required performance specifications. The results of the Phase II prototype field testing will drive the Phase III path toward commercializing a mine detector.

4. Section 1 of the Final Progress Report

4.1 Significant (Key) Findings

The Phase I program resulted in four key findings that underscore the significant impact that the sensor array, algorithms, and wireless mesh network, collectively, would provide toward improving occupational safety and health of mine workers. Specifically, SRD was able to:

1. Synthesize selectively, sensitive SMO sensors capable of detecting the target gases at the concentration ranges typically present in underground mining operations,
2. Develop algorithms capable of interpreting the "raw" sensor array response signals to detect, identify, and quantify each of the four target gases,
3. Adapt the sensor array technology to incorporate the necessary filtering and wireless capabilities for robust and networked operation within typical mining environments, an
4. Demonstrate that sensor array, when coupled with the algorithms, can autonomously and continuously detect, identify, and quantify impending mining hazards to provide early warning to protect mine workers.

SRD evaluated novel, metal-oxide/catalyst doped sensor coatings from its materials library and synthesize new sensing materials for selective identification of the mine relevant target gases. Materials were evaluated based on response time to the analytes, recovery time, response kinetics and thermodynamics, and uniqueness of the dynamic response curves. SRD exposed the sensor array to gas scenarios that simulated two mining conditions including sudden release of a mine gas via a gas pocket and gradual release of gas from fissures or from daily exposure. To focus on an early warning detector, gas testing focused on low, high and critical levels for each mining gas. The sensor array response kinetics was rapid, reversible, sensitive, quantitative, and selective to particular mine gases. These fundamental sensor array response characteristics provided the critical input information to the algorithms.

SRD used the sensor array response data, obtained from all gas testing protocols for both scenarios (sudden change and gradual ramp profiles), to implement a hierarchical algorithm approach to first detect, then identify, and finally quantify the mine gases present in the environment. In particular, key sensor array response features such as rates of responses and recoveries, response magnitudes, and baseline trends were used for refine the hit detector, train the classifier, and calibrate the quantifier or concentration estimator. The sensor array response data is continuously processed (1 Hz data rate) by the hit-detection algorithm whose function is to monitor if any threats are encountered (i.e. target gases are present). If the algorithm detects an event, it extracts key features of the response and invokes the classification algorithm. The classification algorithm is the second stage of the process. Its main job is to identify an event whenever called into action by the hit-detection algorithm. Once the classification algorithm identifies the gas, it invokes the quantitation algorithm. The quantitation algorithm takes the output of the hit-detection algorithm (key features of response) and classification algorithm (identity of gas), uses this information to provide estimates of the concentration of gas.

SRD also integrated and verified a gore water/particulate filter along with a custom flame arrestor to mitigate harsh, and potentially explosive, conditions within mines. SRD also evaluated and verified that a commercial off the shelf (COTS) 900 MHz wireless module demonstrated superior transmission range and was successfully implemented to form a 4-node mesh network that extends wireless transmission range. It is anticipated that a larger mesh network would relay sensor array data to a single base station from any point within a mine, allowing the mine to be chemically mapped and monitored for impending dangerous conditions.

The Phase I performance metrics of the sensor array, coupled with algorithms, was determined including detection times (10-30 seconds), precision (76.7-97.5%), accuracy (87.8-97.7%), and Probability of False Alarms (0-5.5%). The Phase I sensor array and algorithms operated autonomously, without any calibration, while providing precise and accurate detection, identification, and quantification of each mine gas within seconds with no false alarms except for lower CO_2 levels.

4.2 Outcomes / Impact

SRD's Phase I mine detector has demonstrated all the necessary major components that, once developed into a fully integrated Phase II prototype mine detector, will enable any given mine to be chemically mapped continuously and in real-time. The concept involves equipping each mine worker with SRD's wearable mine detector and, in addition, strategically locating detectors on machinery and critical points within the mine. The distributed network of SRD mine detectors, each capable of wireless communication to the base station, would autonomously and continuously report gas conditions and location to provide a true early warning system against impending hazardous mine gas conditions prior to posing any actual danger to mine workers. With the base station receiving early warning alerts of every impending hazardous mine condition along with precise location, it will be possible to alert mine workers and direct them through a safe evacuation route.

In Phase I, SRD has established the necessary technical foundation to build upon in Phase II to focus on designing, constructing, verifying, and field-testing prototype mine detectors. The Phase I results demonstrate the sensor array, algorithm, and wireless mesh network, will dramatically improve occupational safety and health of mine workers by chemically mapping the entire mine to provide early warning of possible explosive conditions. The base station will receive early warning of impending threats and precise locations to allow mine workers to be directed through a safe evacuation route. SRD's mining detectors will be low-cost (~$500-$750) and small enough to wear or carry and be mounted in fixed locations or on machinery. Each detector will have integrated wireless transmission communications and support real-time, continuous self-diagnostics to extend operational lifetime. The simple power ON / power OFF detector operation will not require any calibration, saving mine workers time to focus on other safety gear.

In Phase II, SRD will construct, verify, and field test prototype mine detectors in two separate field test trials, within an active mine, for a spiral development to ensure the prototype mine detectors meet the required performance specifications. The results of the Phase II prototype field testing will drive the Phase III path toward commercializing a mine detector.

5. Section 2 of the Final Progress Report

5.1 Scientific Report

In the scientific report, Sensor Research and Development Corporation (SRD) SRD provides a brief background for the project, lists the specific aims, describes the methodology or technical approach, presents the Phase I results with discussion, and summarizes the Phase I conclusions. The background for the project, specific aims, methodology sections summarize key information from within the Phase I proposal while the results and discussion and conclusion sections present and analyze the progress made during the entire Phase I program.

5.1.1 Background for the Project

SRD brought to this program a unique, versatile nano-sensor technology that is designed for continuous, real-time detection, monitoring, and analysis of atmospheric gases in adverse conditions. SRD's sensor technology has been developed, tested and verified by independent laboratories through support of the Department of Defense, the Department of Homeland Security, the Office of Naval Research, and the Department of Energy. The foundation of SRD's chemical detection system is a monolithic complementary metal–oxide–semiconductor (CMOS) micro-hotplate sensor array which currently supports 16 nano-sized SMO sensors, each coated with a chemically tailored, analyte selective, catalyst doped metal oxide sensing film. By incorporating up to 16 selective gas sensors into a miniature sensor array, SRD can detect, monitor and quantitatively analyze the chemical components of complex atmospheric gas mixtures within diverse gas backgrounds. SRD has successfully developed and field-tested handheld and lightweight portable detectors having the ability to routinely detect, identify, and quantitate toxic industrial chemicals (TICs) and chemical warfare agents (CWAs) at permissible exposure levels (PELs) and immediately dangerous to life and health (IDLH) levels (parts-per-trillion to parts-per-million), in diverse backgrounds and widely variable environmental conditions.

The application of SRD's sensor array technology toward the analysis of atmospheric gases was proven through third-party evaluation and field-testing under extreme environmental conditions of 210 °C and 95% relative humidity in the analysis of coal fired power plant combustion emission gases (NETL project, 2007). SRD demonstrated the ability to accurately and reliably monitor gases directly relevant to the proposed effort and did so under extremely harsh and abnormal environmental conditions. The field test included the following gases: nitric oxide (NO), nitrogen dioxide (NO_2), ammonia (NH_3), hydrogen sulfide (H_2S), sulfur dioxide (SO_2), carbon monoxide (CO) and carbon dioxide (CO_2). During the NETL project to flue-gas components, the probability of a false alarm (PFA) was 3.5% due to misclassification, there were 0% false negatives, and there were 0% nuisance alarms.

SRD's goal in this Phase I program was to demonstrate that our proven, field-tested sensor technology, a micro-array of micro-electromechanical system (MEMS)-based semiconductor metal-oxide (SMO) environmental gas and chemical sensors, can be used to detect and analyze

coal mine atmospheric gases. Most importantly, through continued development efforts, the sensor array will be integrated into a predictive atmospheric gas modeling system, capable of early identification and warning of an impending risk of explosive and auto-ignition conditions within the mine.

This multi-gas detector will be deployable as a cross-functional monitor (machine mounted, hand-held, wearable, and/or stationary detector incorporated into an extensive wireless atmospheric monitoring system (AMS)), thereby replacing, through consolidation, all of the gas monitors currently used inside the mine. All the application specific multi-gas detectors used throughout the mine will have a common architecture – the 16-sensor micro-array, the associated electronics, and embedded software – allowing the creation of a multi-functional sensor network, greatly simplifying (from an equipment and users perspective) the gas detection methodologies currently used in mining operations. The stationary atmospheric gas detectors could be incorporated into a sophisticated fully integrated AMS, with each sensing array networked wirelessly (for example, using the Wireless Mesh Mine Communication System developed by L-3 Communications (with whom we have a commercialization agreement), or the ActiveMine System, manufactured by Active Control Technology Inc.) and linked to a command center above ground. The ultimate goal of this applied research is the commercialization of a comprehensive multi-gas analyzer, suitable for stationary, portable and machine mounted applications with the necessary support electronics and software enabling complete wireless data transfer to remote control centers to essentially chemically map the entire mining area continuously and in real-time.

SRD has developed a sensor array capable of real-time, continuous atmospheric monitoring of methane while simultaneously monitoring the key atmospheric gases recognized as predictors and indicators of spontaneous combustion and coal self-ignition. In this Phase I effort, SRD focused on the detection and quantitation of methane (explosive, asphyxiant), carbon monoxide (combustion gas, asphyxiant), oxygen (atmospheric gas), and carbon dioxide (combustion gas, asphyxiant). These gases were selected based on their importance in establishing the status and safety of the mine atmosphere. Current analytical methods rely on gas chromatography and handheld monitors to obtain the target gas concentrations. Both of these approaches require an operator to be at the sampling location, which in many cases is not possible due to the safety risk or inability to simultaneously monitor multiple locations. Advancement of a multi-gas, cross-functional, atmospheric gas sensor array, adaptable to the development of machine mounted detectors, hand-held gas detectors, and fixed-position, stationary gas analyzers, will greatly improve the safety of current mining operations while lower the operational costs. The use of sensitive, real-time, self-calibrating, selective gas sensors linked within a unified distributed sensor network will provide the mining industry greater understanding of the atmospheric conditions throughout the mine, in both actively mined and inactive locations. The captured data will allow the continued development of predictive tools based on established fire-related equations.

5.1.2 Specific Aims

SRD used the Phase I research and development effort to develop and demonstrate an array of miniature gas sensing elements that, when coupled with appropriate algorithms, can detect and

monitor the explosive and toxic gases frequently encountered in coal mine atmospheres. This was accomplished through semiconductor metal-oxide thin film materials development, miniature sensor array fabrication, target chemical gas delivery and verification testing, and software algorithm design and implementation. The two major objectives of the proposed solution were:

1) Develop a solid-state sensor array capable of real time *in situ* detection and monitoring of relevant coal mining gases
2) Demonstrate solid-state sensor array performance in simulated mine background conditions (ambient temperature, relative humidity, atmospheric gases – using Gaussian-like exposures)

The relevant concerns and technical questions related to these objectives were:

1) Can SRD's extremely sensitive SMO sensors be used to detect the target gases at the concentration ranges that are typically present in underground mining operations?
2) Can algorithms be developed to quantitate the target gases within the precision requirements demanded by this application?
3) Can SRD's current technology be adapted to incorporate the necessary filtering and wireless capabilities for typical mine-like operations?

SRD evaluated novel, metal-oxide/catalyst doped sensor coatings from its materials library and synthesize new sensing materials for selective identification of the mine relevant target gases. Materials were evaluated based on response time to the analytes, recovery time, response kinetics and thermodynamics, and uniqueness of the dynamic response curves. Sensor arrays were constructed and evaluated using advanced signal processing methods, for the detection and identification of methane, carbon monoxide, oxygen, and carbon dioxide in background atmospheres simulating the mining environment.

There are four milestones that were used to gauge SRD's performance during the Phase I effort:

1) Synthesize and select a solid-state sensor array for the selective detection of methane, carbon monoxide, oxygen and carbon dioxide
2) Challenge the sensor array to combustion and atmospheric gases in simulated coal mine conditions
3) Develop algorithms based on sensor array response kinetics
4) Validate sensor array with embedded algorithms to confirm/determine the detector's performance

5.1.3 Methodology

The Phase I effort demonstrated the successful design and implementation of a solid-state sensor network capable of *in situ* operation and the real-time, selective detection of the combustion gases methane (CH_4) and carbon monoxide (CO), and atmospheric gases oxygen (O_2) and carbon dioxide (CO_2) in the presence of typical mine-like background conditions (relative humidity of 80% and ambient temperature of 10 °C). At the end of Phase I, SRD demonstrated the sensor

network's ability to detect the target gases at the following concentration ranges: methane (0.1% to 1.0%), carbon monoxide (10 ppm to 1200 ppm), oxygen (10% to 25%), and carbon dioxide (0.1% to 1.0%). The proposed Phase I goal and technical objectives were achieved by executing the following six major tasks:

1. Synthesize and select an array of SMO sensors to detect combustion gases CH_4 and CO, and monitor atmospheric gases O_2 and CO_2,
2. Challenge the sensor array to the test matrix of combustion and atmospheric gases,
3. Evaluate filters and flame arrestor techniques capable of integration into current technology for mining applications,
4. Develop sensor array signal processing algorithms based on sensor array response characteristics to simulated mine conditions,
5. Establish the basis for a wireless sensor network (WSN) for real-time monitoring for potential fires or hazardous conditions within a mine, and
6. Verify operation and determine performance metrics of sensor array when coupled with embedded algorithm.

A brief description of each of the six tasks is provided in this section. Details of the actual work performed is provided in the "Results and Discussion" section.

Task 1: Synthesize and select an array of SMO sensors to detect combustion gases CH_4 and CO, and atmospheric gases O_2 and CO_2

SRD's semiconductor metal-oxide (SMO) sensors are thin-film transition-metal-oxide/catalyst-doped chemiresistive sensors. SRD has miniaturized its sensor platform so that 16 chemically-tailored selective sensors are arranged with in a 4 x 4 orthogonal sensor array with a total area of 2 mm x 2 mm. The chemo-selective sensor films (100 μm x 100 μm) are formed from the SMO suspensions deposited onto the platforms using picoliter-dispensing technology. The benefit of this sensor array approach, as opposed to discrete single gas sensors, is these SMO films undergo predictable and reproducible redox reactions that, when incorporated into a multi-sensor array, provide a dynamic pattern which can be used to monitor multiple gases simultaneously. Another advantage to the sensor technology developed by SRD is the flexibility to design the sensor arrays to accurately detect and identify all atmospheric agents that can provide an early warning for the conditions that increase risk of explosion and/or fire as well as when atmospheric conditions within the mine maybe hazardous to workers.

SRD has synthesized and experimentally characterized unique, specific and selective SMO materials for chemical detection. The library of SMO coatings and gas testing database includes over one million gas exposure responses and was used to initiate the selection process in designing a sensor array for the four targets (CH_4, CO, O_2 and CO_2) of the Phase I effort. Additional sensing materials were synthesized, characterized and evaluated in the sensor array against the target gases. SRD employed an iterative approach to refine and improve each SMO sensor coating based on the mechanistic theory of operation, comparison to the performance of SRD's existing library of materials, and the empirical data obtained in this program. SRD has

synthesized metal oxide based SMO coatings that are selective to the Phase I target gases. These materials were evaluated and optimized to meet the objectives of this program.

SRD has developed emulsion-based synthetic methods using Sol-Gel technology to prepare nano-sized metal oxides using tungsten oxide (WO_3), tin oxide (SnO_2), indium oxide (In_2O_3), and a variety of mixed metal-oxide materials for the selective detection of CH_4, CO, O_2 and CO_2 (Figure 1). The nano-sized materials are necessary to enhance the sensors' sensitivity to ppt levels and ensure sensor-to-sensor reproducibility. The synthetic conditions – reaction temperature, reaction time, chelating agents, starting materials, and catalysts for condensation at low temperature – are optimized for each unique sensing material.

Figure 1: Schematic drawing of SRD's metal-oxide powder synthesis method

Task 2: Challenge the sensor array to the test matrix of combustion and atmospheric gases

SRD subjected their candidate SMO nano-sensors *and* final sensor array, developed in Task 1, to a range of gas test protocols exposing the sensors to CH_4, CO, O_2, and CO_2, at 80% relative humidity (RH). The initial candidate sensors were screened for a range of concentrations (see Table 1) at standard operating conditions. Standard environmental conditions are defined as 80% RH, 20 °C (room temperature) and a pressure of 1 atm. The standard chemical background condition was established as 20.0% O_2 and 0.01% CO_2 in 80% RH.
Table 1 lists the high and low concentration ranges SRD used in the tests and also lists the critical gas concentrations. For CH_4, 1.0% is the critical concentration where all the electrical equipment and machinery are turned off in order to avoid possible explosive conditions. Typically, 0.5% is used as the first warning alarm level. Carbon monoxide levels were chosen at the NIOSH and OSHA alarm levels. The critical gas concentration for O_2 was chosen based on NIOSH's low working alarm level. Carbon dioxide critical levels were chosen based on NIOSH TVL/PEL levels.

To execute Task 2, SRD made key modifications to one of their existing gas delivery systems to handle all four target gases and their respective concentration ranges with the capability to control background relative humidity levels. Certified compressed gas tanks at different

concentrations were obtained for delivering the wide range of gases proposed in the Phase I effort. Modifications to the existing gas delivery system included additional support for target gases in their appropriate concentration ranges, addition of a humidity controller with feedback loop, and also the ability to test gases at 10 °C and 20 °C (room temperature). An environmental chamber was also incorporated to achieve the desired temperatures and a humidity bubbler will be used to generate water vapor in the delivery system.

Table 1: Concentration of analytes used for screening

Chemical Analyte	High Concentration	Low Concentration	Critical Gas Concentrations
Methane	1.0%	0.1%	0.5% low alarm 1.0 % shut off alarm
Carbon Monoxide	1200 ppm	10 ppm	35 ppm NIOSH alarm 50 ppm OSHA alarm
Carbon Dioxide	1.0%	0.1%	0.5% PEL Level
Oxygen	22.0%	18.0%	19.5% NIOSH low working alarm

The gas test protocols performed during Phase I are detailed in the Results and Discussion section along with the corresponding SMO sensor array results. SRD used certified gas cylinders as the supply sources for each of the four target gases. A Shimadzu gas chromatography mass spectrometer (GC/MS) was also used to provide ground truth validation of the gas delivery system for CH_4 at low levels and gas chromatography flame ionization detector (GC/FID) was used at higher concentrations. Ground truth validation for CO, O_2, and CO_2 was achieved using the GC/MS along with a gas chromatography thermal conductivity detector (GC/TCD) for higher concentrations. Concentrations specified on the certified standard tanks were used as the primary calibration standards. SRD also simultaneously tested and validated a commercial off the shelf (COTS) devices for direct comparison with SRD's SMO sensor array. Gas sensor test results were used in Task 4 to optimize the sensor array signal processing algorithms and to steer any SMO sensor array modifications.

Task 3: Evaluate different filtering and safety techniques capable of integration into current technology for mining applications

The majority of mining applications require gas-sampling systems to operate in harsh environmental conditions. The harsh environmental conditions include extremely high relative humidity (80%), low temperatures (10 °C), diesel particulate matter, as well as dust/rock particulate matter. In order to increase the robustness of SRD's current solid-state sensor array technology, various filtration techniques were considered for protecting the sensing element. Humidity, diesel particulates, and dust particulate matter are targeted contaminates in the filtration evaluation. SRD determined that the GORE Protective Vents provide an effective barrier against harsh environmental conditions, such as driving rain, dust, and dirt.

When monitoring for explosive gases, such as methane, the detectors must remain intrinsically safe to protect the mine as well as the mineworkers. Safety is of extreme importance to both the staff at SRD as well as NIOSH. SRD's development staff has investigated flame arresters to ensure the safety of their solid-state sensor array technology. A flame arrester is installed to stop the propagation of a deflagration traveling along a pipeline by extinguishing the flame. The principle of a flame arrester operation is forcing a flame front through channels too narrow to permit the continuance of a flame.

Task 4: Develop sensor array signal processing algorithms based on sensor array response characteristics

SRD has developed a highly robust signal processing architecture of integrated algorithms capable of detecting, identifying, and quantifying mining gases over key concentration ranges using the "raw" SMO sensor array response signals. The architecture requires no calibration procedures, as the algorithms are autonomous and adaptive. Upon start-up, the algorithms measure the sensor array's baseline signals and automatically adjust its parameters. The algorithms continue the self-adjustment in an adaptive manner throughout its operation. Due to the self-calibration capabilities and adaptive behavior, all modifications to the algorithms development were focused on the following major areas:

1. Hit-detection
2. Classification
3. Quantitation

These algorithm details along with their results are presented in the Results and Discussion section.

Task 5: Development of a wireless sensor network (WSN) for real-time monitoring for potential fires or hazardous conditions within a mine

There are currently a handful of manufacturers that support data and voice communication that are approved by MSHA to work within mines. The type of transmission used in these systems, in most cases, is split between hardwired and wireless networks. The most common hardwired system used is the so-called "Leaky Feeder" system. This system has been the primary communications system in mines, mass transit underground tunnels and railway systems for a number of years. Although a proven technology, the limitations of this system are:

- High installation and maintenance cost
- As mines are extended, the Leaky Feeder cable and supporting hardware is not always installed until much later due to installation issues
- Cave-ins will likely cause disruption of Leaky Feeder cable service to critical areas

To help alleviate most of these limitations, numerous manufacturers continue to develop communication systems that rely totally on wireless technologies that are networked together

into a meshed topology. These wireless mesh networks (WMN) operate by allowing individual nodes to communicate dynamically with multiple nodes within the mesh, therefore providing a robust and self-healing system that automatically re-routes around a node that drops out due to loss of signal, operation or performance. This allows the network to remain intact and operational providing a reliable continuous communication of the mine conditions including any alarms.

There are a number of WMNs presently being used within mines. For example, one such mesh network utilizes MSHA approved ActiveMine RFID Wi-Fi tags, which are manufactured by Active Control Technology Inc. This network of wireless routers allows equipment and miner tracking in real-time and data and voice communication. Another system currently in final development is the Wireless Mesh Mine Communication System manufactured by L-3 Communications Global Security & Engineering Solutions (L-3 GS&ES, whom SRD has a commercialization partnership with). This system also uses a mesh network, but relies on an ideal frequency that does not require line-of-sight. This system will also support real-time tracking of equipment, miners, data, and voice communication.

SRD tested and evaluated different wireless technologies out of line-of-site communication. Additionally, unique identifiers were assigned, using a Media Access Control (MAC) address, to each sensor node within a hybrid network. SRD evaluated transmission frequencies of 315 MHz, 900 MHz, and 2.4 GHz. Each of these three operating frequencies was evaluated in different operating conditions to determine the maximum transmission distance (MTD). The different conditions include:

- In a clear line-of-site (under different outdoor atmospheric conditions – relative humidity and temperature will be noted)
- Inside a metal-framed building (in different rooms, different sized-rooms, hallways, etc.)
- In a wooded area (no direct line-of-site with many natural obstructions).

Each of the conditions was also evaluated using multi-nodal meshed communications.

Task 6: Validate sensor array with embedded algorithm for feasibility study

SRD evaluated the performance of the sensor array coupled with the signal processing algorithms to determine the following performance metrics:

- Probability of False Alarm (PFA)
- Lower Limit of Detection (LLOD)
- Accuracy of Quantitation

Data obtained from exposing the sensor array to the target gases (Task 2) were autonomously processed using the signal processing algorithms developed in Task 4. The performance metrics of the Phase I sensor array, coupled with algorithms, are detailed in the Results and Discussion section.

5.1.4 Results and Discussion

In this section, SRD details all of the Phase 1 results. The results are presented in six different subsections where each subsection corresponds to one of the six program tasks. Based on the progress and results, SRD is able to clearly demonstrate that the Phase I program objectives, technical questions, and milestones has been achieved and/or addressed.

As a reminder, the two Phase I objectives were:

1) Develop a solid-state sensor array capable of real time *in situ* detection and monitoring of relevant coal mining gases and
2) Demonstrate solid-state sensor array performance in simulated mine background conditions (ambient temperature, relative humidity, atmospheric gases – using Gaussian-like exposures).

The three Phase I technical questions that were answered include:

1) Can SRD's extremely sensitive SMO sensors be used to detect the target gases at the concentration ranges that are typically present in underground mining operations?
2) Can algorithms be developed to quantitate the target gases within the precision requirements demanded by this application?
3) Can SRD's current technology be adapted to incorporate the necessary filtering and wireless capabilities for typical mine-like operations?

The four milestones that SRD accomplished during the Phase I effort include:

1) Synthesize and select a solid-state sensor array for the selective detection of methane, carbon monoxide, oxygen and carbon dioxide,
2) Challenge the sensor array to combustion and atmospheric gases in simulated coal mine conditions,
3) Develop algorithms based on sensor array response kinetics, and
4) Validate sensor array with embedded algorithms to confirm/determine the detector's performance.

The following six program tasks provide the outline for the six subsections to report Phase I progress and accomplishments within the Results and Discussion section:

1. Synthesize and select an SMO sensor array to detect mining gases,
2. Challenge the sensor array to mining gases,
3. Evaluate filters and flame arrestor techniques,
4. Develop sensor array signal processing algorithms,
5. Establish the basis for a wireless sensor network (WSN), and
6. Verify operation and determine performance metrics of sensor array with algorithms.

5.1.4.1 Synthesize and select SMO sensor array to detect & monitor mining gases

SRD synthesized a range of SMO nano-sensors, each with different chemical and physical properties toward selective detection of CH4, CO, O2, and CO2. Specifically, SMO nano-clusters were synthesized while progressively encapsulating each cluster with appropriate catalysts to target faster response kinetics with a particular target gas (i.e. CH4, CO, O2, and CO2). SRD focused their SMO nano-cluster chemistries based on:

- Lewis acid chemistry,
- Oxidation potentials, and
- Diffusion characteristics within the SMO surface reaction zone.

An example of SRD's synthetic strategy to select and develop sensing materials for a methane sensor is detailed. Typical metal oxide materials such as SnO_2, ZnO, In_2O_3 and WO_3 doped with noble metal catalysts such as gold (Au), platinum (Pt) and palladium (Pd) are good candidates for sensing materials that will demonstrate enhanced sensitivity and selectivity toward methane (CH_4).

The SMO chemiresistive sensing mechanism for CH_4 is based on changes in the electrical resistance of highly porous SMO thin films due to two main reactions occurring at the surface. In the first reaction, atmospheric oxygen molecules are chemically adsorbed at specific sites of the oxide surface. They are ionized to O^-_{ads} by accepting an electron from the metal oxide conduction band. This reaction leads to an increase in SMO film resistance. The descriptive equation is:

$$O2 + 2e- \rightarrow 2O^-_{ads}$$
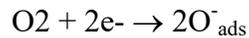
In the second reaction, CH_4 reacts with the chemisorbed oxygen to donate an electron back to the conduction band, thus decreasing the SMO resistance, as described in the next equation:
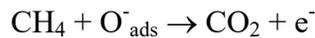
$$CH_4 + O^-_{ads} \rightarrow CO_2 + e^-$$

To convert reactants into products, in the reaction $CH_4 + O^-_{ads} \rightarrow CO_2 + e^-$, the reactants must overcome the activation energy of the reaction, as shown in Figure 2. The lower activation energy barrier, the higher conversion ability (faster reaction rate) leading to product, and the sensor response will be higher. As shown in Figure 2, catalysts can lower the activation energy barrier of reaction significantly. In this case, the sensitivity to CH_4 will be increased.
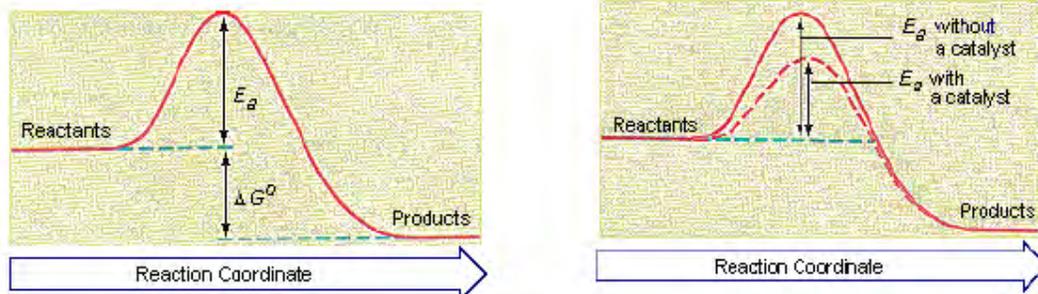
Figure 2: Activation energy curve for CH₄ oxidation reaction (with and without catalyst)

Of the candidate SMO materials that SRD synthesized and screened, five (5) SMO sensors were selected for their exceptional ability to detect, identify, and quantify the mine gases including methane (CH_4), carbon monoxide (CO), carbon dioxide (CO_2) and oxygen (O_2). These five SMO sensors along with their operating temperatures, and dominant gas responses, are listed in Table 2. These five sensors comprise the sensor array that the algorithms, in Task 4, were optimized around and the performance metrics summarized in Task 6.

Table 2: Sensor array materials selected to target CH₄, CO₂, CO and O₂.

Number	Material	Temperature (°C)	Chemical Detection
1	SnO2+0.8%Pd	200	CO, CO_2
2	SnO2+10%La	550	CO, CH_4
3	SnO2+2%La	550	-
4	ZnO+5%Pt	400	CH_4, O_2
5	In11.3SmO18.5	200	CO_2, O_2

All five sensors in the array were subjected to different concentrations of each of the four mining gases to gauge their selectivity toward each of the gases. Figure 3 shows the Fisher's linear discriminant analysis (LDA) output for the four target gases. This plot is the visualization of the resolution ability of a five dimensional (five sensor array) data in the three dimensional space representation. The dimensional reduction is achieved by using Fisher's LDA approach which tries to model the differences between the sensor array's responses to the each of the target gases. The solid red balls indicate normalized response of the sensor array to different concentrations of CH_4, the solid blue balls are normalized response to varying concentrations of CO, the solid green balls are normalized response to varying concentrations of O_2 and the solid black balls are normalized response to varying concentrations of CO_2.
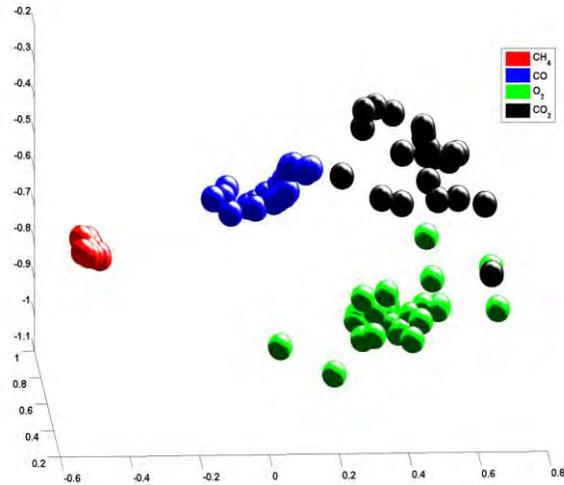
17

Figure 3: Linear discriminant analysis plot of the Sensor Array's responses to each target gas at relevant concentrations demonstrating the desired separation of response characteristics needed to distinguish between each gas.

The LDA plot demonstrates that the five sensor array's response signals can be used to distinguish between the four target gases as evidenced by the clustering of the responses for the same gas and the separation of clusters between each of the four gases. SRD also provides spider charts in Figure 4 that represents the normalized response magnitude at a given point in time for each of the five sensors, hence five-vector spider charts. The spider charts represent the five-sensor array's response patterns to each of the four mine gases after 200 seconds of a 300-second gas exposure for each of the target gases. The red spider chart (upper left) represents the sensor array's response pattern to methane, whereas the blue spider chart (upper right) represents the sensor array's response pattern to carbon monoxide. The black spider chart (lower left) represents the sensor array's response pattern to oxygen, while the green spider chart (lower right) represents the sensor array's response pattern to carbon dioxide. The spider charts are another effective tool, along with the LDA plot, to graphically demonstrate the sensor array's clear ability to distinguish between each of the four mine target gases. It is important to note that SRD is only using LDA and spider charts as graphical representations to illustrate the selectivity of the five sensor array. However, the gas identification algorithms, developed in Task 4, are much more powerful methods for using the Sensor Array's response kinetics to identify the gas present.
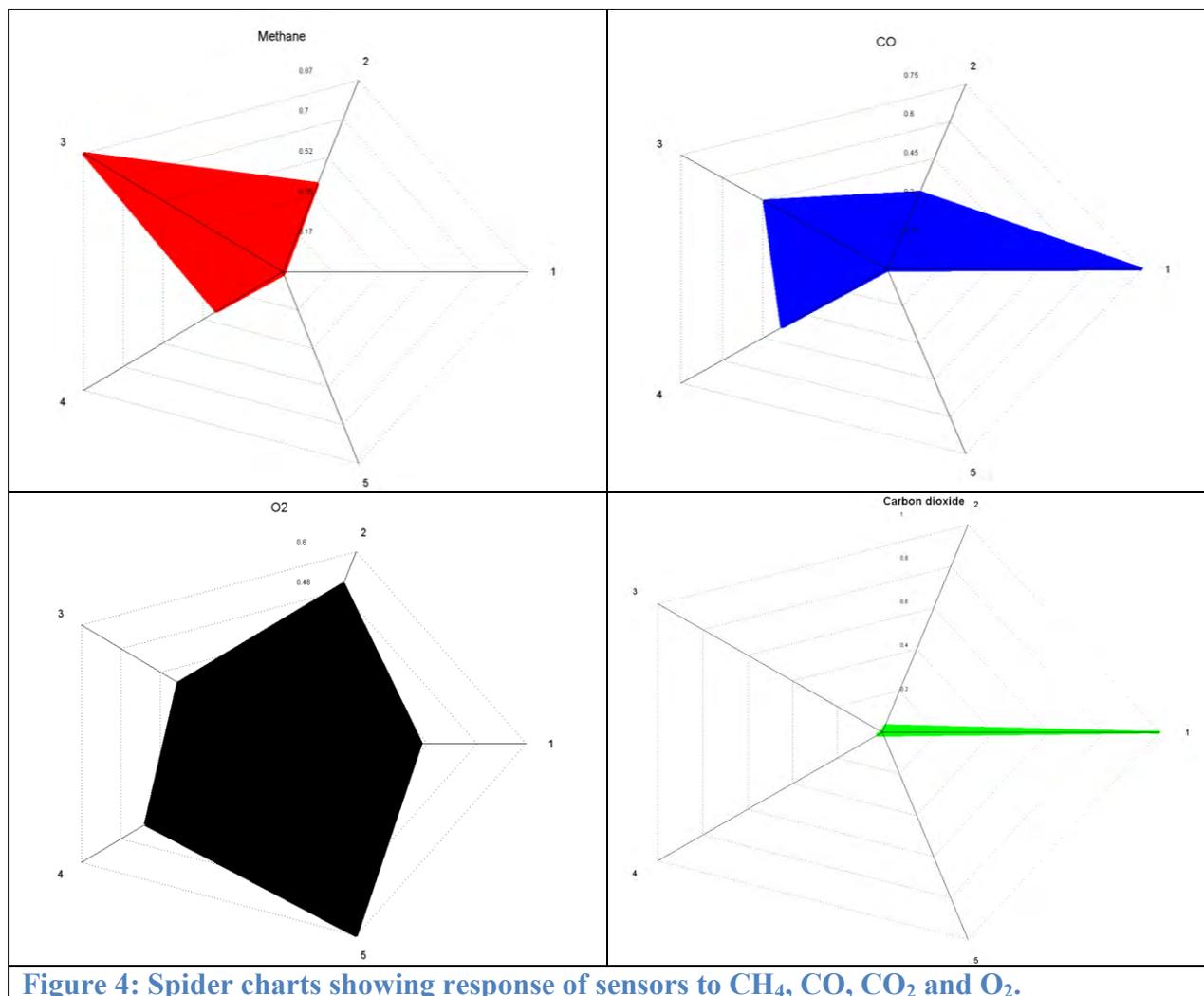
Figure 4: Spider charts showing response of sensors to CH₄, CO, CO₂ and O₂.

The four spider charts, shown in Figure 4, demonstrate that only sensors 2, 3, and 4 respond to methane while only sensor 1 responds to carbon dioxide. Sensor 5 does not respond to carbon monoxide, while all sensors respond to oxygen. These key sensor characteristics are valuable in not only being able to detect all four gases, but to distinguish between the gases.

SRD uses spider charts again, in Figure 5, to compares the sensor array's responses to 0.12 ppm of methane gas at after three different exposure times including 25, 60, and 300 seconds, respectively. By the similar response patterns from each of the three exposure times, it is evident that the sensor array's response pattern at 25 seconds is sufficient to detect and identify methane. Figure 6 compares the spider charts of the sensor array's normalized response patterns to methane gas after 25 seconds of exposure to three different concentrations including 0.12 ppm, 0.5% and 1200 ppm, respectively. These results indicate that the sensor array could detect and identify methane gas, independent of concentration, which significantly simplifies gas identification with multiple target gases simultaneously present. It is important to note that these results were normalized, thereby factoring out concentration effects. The five sensor array has demonstrated a clear capability to provide quantitative measurement of each of the four target gases (detailed with results in subsections 5.1.4.4 and 5.1.4.6).
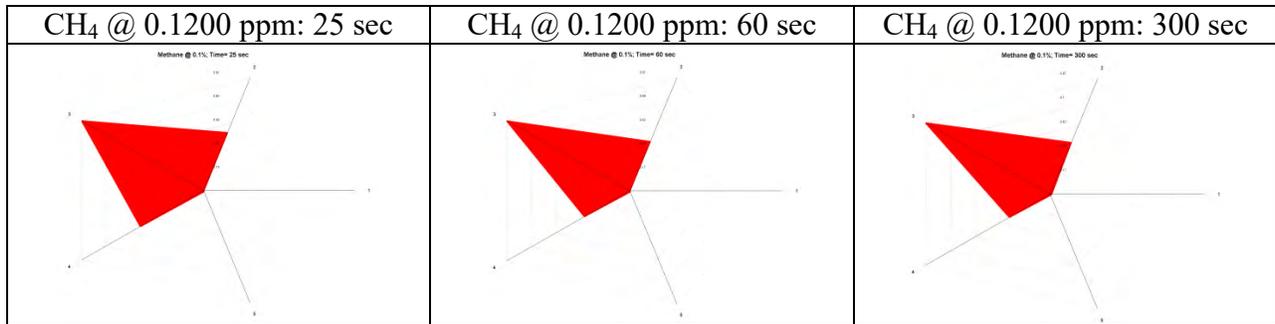
CH$_4$ @ 0.1200 ppm: 25 sec	CH$_4$ @ 0.1200 ppm: 60 sec	CH$_4$ @ 0.1200 ppm: 300 sec

Figure 5: Spider charts of Sensor Array response patterns to 0.12 ppm CH$_4$ as a function of exposure time.

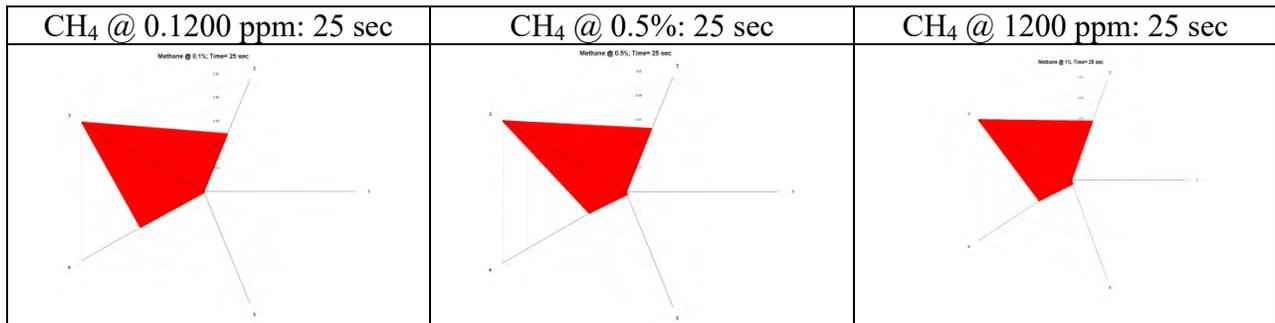| CH$_4$ @ 0.1200 ppm: 25 sec	CH$_4$ @ 0.5%: 25 sec	CH$_4$ @ 1200 ppm: 25 sec

Figure 6: Spider charts of Sensor Array response patterns for 3 CH$_4$ concentrations after 25 seconds of exposure.

Like the results presented for methane, Figure 7 compares the sensor array's normalized responses to 100 ppm of carbon monoxide gas at after three different exposure times including 25, 60, and 300 seconds, respectively. By the similar response patterns from each of the three exposure times, it is evident that the sensor array's response pattern at 25 seconds is sufficient to detect and identify carbon monoxide. Figure 8 compares the spider charts of the sensor array's normalized response patterns to carbon monoxide gas after 25 seconds of exposure to three different concentrations including 100 ppm, 600 ppm and 1200 ppm, respectively. These results support the same conclusions as previously made for methane that the sensor array responds well within 25 seconds and can identify carbon monoxide against the other mine gases independent of concentration levels.
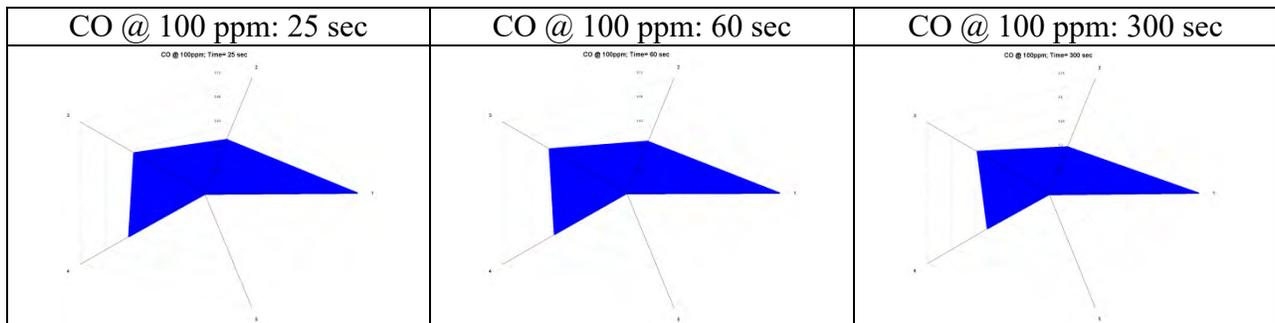
CO @ 100 ppm: 25 sec	CO @ 100 ppm: 60 sec	CO @ 100 ppm: 300 sec

Figure 7: Spider charts of Sensor Array response patterns to 100 ppm CO as a function of exposure time.

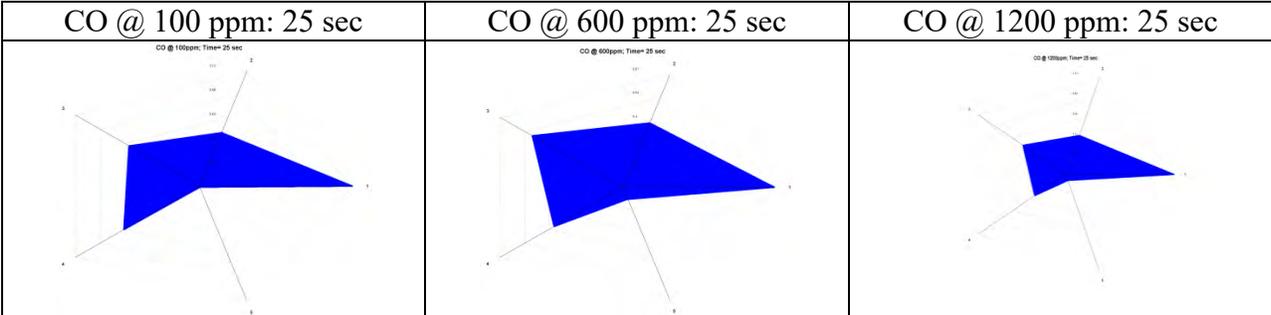| CO @ 100 ppm: 25 sec	CO @ 600 ppm: 25 sec	CO @ 1200 ppm: 25 sec

Figure 8: Spider charts of Sensor Array response patterns for 3 CO concentrations after 25 seconds of exposure.

Like the results presented for methane and carbon monoxide, Figure 9compares the sensor array's normalized responses to 1200 ppm of oxygen gas, above baseline oxygen level of 20.75%, after three different exposure times including 25, 60, and 300 seconds, respectively. By the similar response patterns from each of the three exposure times, it is evident that the sensor array's response pattern at 25 seconds is sufficient to detect and identify oxygen. Figure 10 compares the spider charts of the sensor array's normalized response patterns to oxygen gas after 25 seconds of exposure to three different concentration increases above the baseline oxygen level of 20.75% including 0.12 ppm , 0.5%, and 1200 ppm, respectively. These results support the same conclusions as previously made for methane and carbon monoxide that the sensor array responds well within 25 seconds and can identify oxygen against the other mine gases independent of concentration levels.
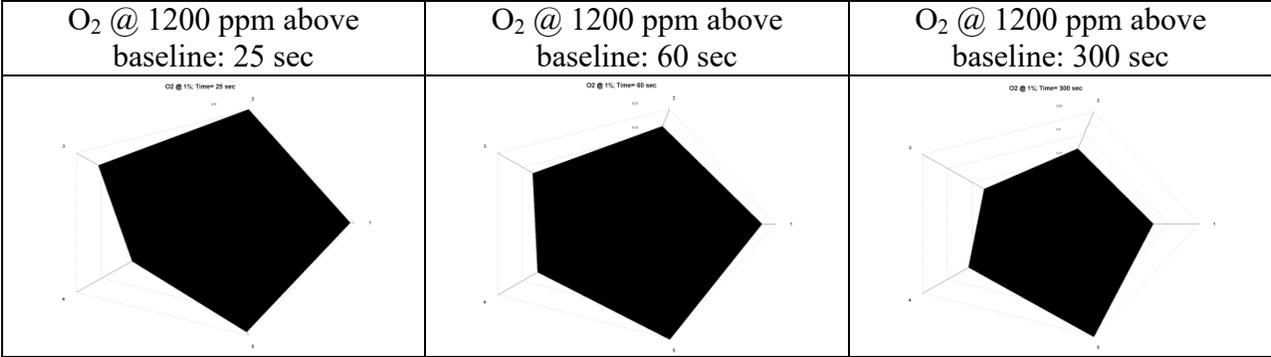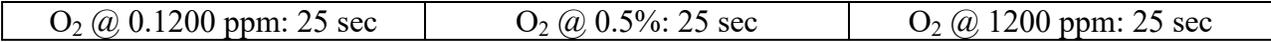
O_2 @ 1200 ppm above baseline: 25 sec	O_2 @ 1200 ppm above baseline: 60 sec	O_2 @ 1200 ppm above baseline: 300 sec

Figure 9: Spider chart response patterns for O_2 at 1200 ppm above baseline conditions of 20.75% O2 as a function of exposure time.

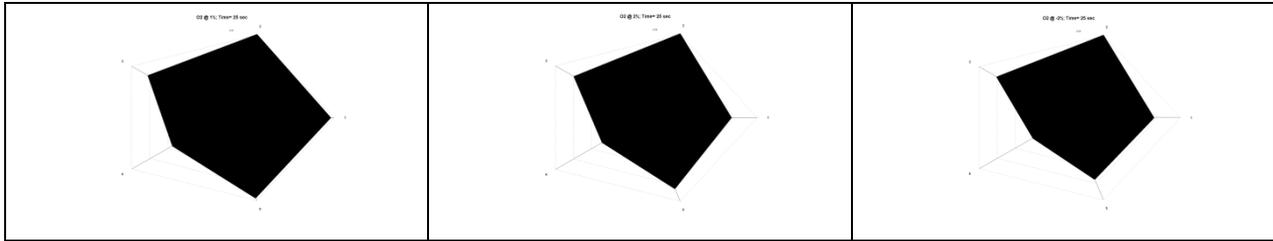| O_2 @ 0.1200 ppm: 25 sec	O_2 @ 0.5%: 25 sec	O_2 @ 1200 ppm: 25 sec

Figure 10: Spider chart response patterns for 3 concentrations of O$_2$ after 25 seconds of exposure.

Like the results presented for methane, carbon monoxide, and oxygen, Figure 11 compares the sensor array's normalized responses to 0.9% carbon dioxide gas after three different exposure times including 25, 60, and 300 seconds, respectively. By the similar response patterns from each of the three exposure times, it is evident that the sensor array's response pattern at 25 seconds is sufficient to detect and identify carbon dioxide. Figure 12 compares the spider charts of the sensor array's normalized response patterns to carbon dioxide gas after 25 seconds of exposure to three different concentration including 0.12 ppm , 0.65%, and 0.9%, respectively. These results support the same conclusions as previously made for methane, carbon monoxide, and oxygen that the sensor array responds well within 25 seconds and can identify carbon dioxide against the other mine gases independent of concentration levels.
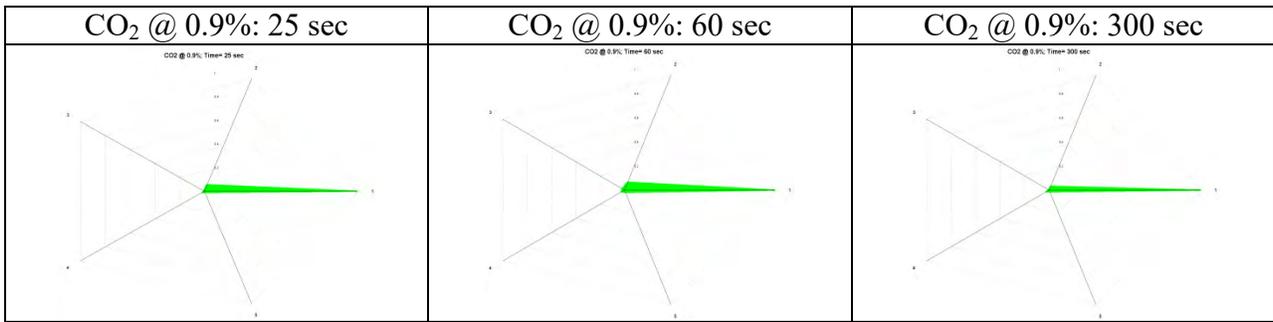
CO$_2$ @ 0.9%: 25 sec	CO$_2$ @ 0.9%: 60 sec	CO$_2$ @ 0.9%: 300 sec

Figure 11: Spider chart response pattern to 0.9% CO$_2$ after 3 different exposure times.

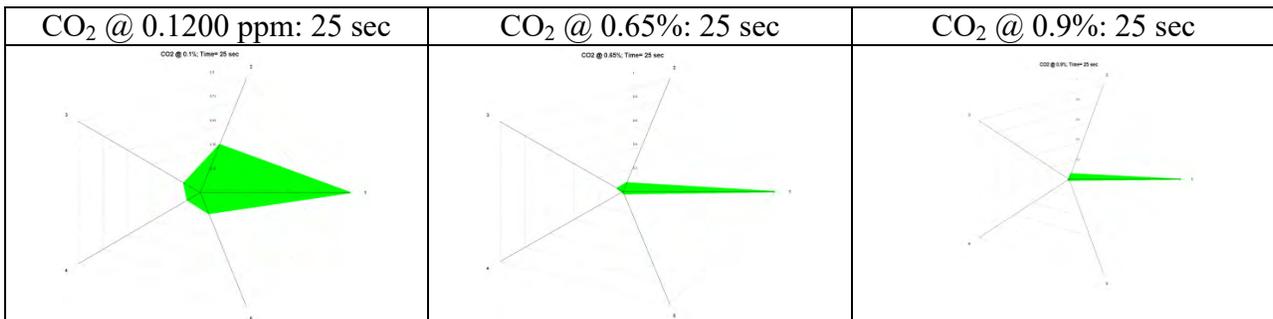| CO$_2$ @ 0.1200 ppm: 25 sec	CO$_2$ @ 0.65%: 25 sec	CO$_2$ @ 0.9%: 25 sec

Figure 12: Spider chart response patterns to CO$_2$ at 3 concentrations after 25 seconds of exposure.

5.1.4.2 Challenge the sensor array to mining gases

This section discusses the efforts taken at SRD to build a gas delivery system to deliver the four mine gases at a variety of concentrations and concentration profiles with specified background conditions. The gas testing protocols used to execute the entire Phase I program is also detailed. SRD also provides details and results pertaining to the ground truth validation of the gas delivery system to support algorithm development in Task 4 and to determine the sensor array's performance metrics in Task 6.

Gas Delivery System:

In order to enable the testing of the four mine gases, SRD developed a gas delivery system to mix and deliver the gases to the SMO sensors. Certified gas cylinders and verified high purity (VHP) oxygen and nitrogen cylinders are connected to calibrated and verified mass flow controllers (MFC). For this gas delivery system, VHP oxygen and nitrogen and certified tanks of 10% carbon dioxide, 1% and 1000 ppm carbon monoxide, 10% methane were used to deliver the Phase I gases. Figure 13 provides a detailed schematic of the gas delivery system designed and built to support all Phase I sensor testing.

As shown in Figure 13, N_2 is passed through the mixing chamber where CO (low and high), CO_2, CH_4 are combined and mixed. While analyte gases are mixing, separate N_2 gas stream and O_2 gas stream are mixing to deliver the correct O_2% for the tests. This is stream is passed through the water bubbler to mix and provide the correct humidity. This resultant gas stream is then combined with the analyte gas stream to produce the final gas mixture. This gas stream is set to have a 1 L/min total flow. The MFCs are controlled via a computer such that precise (1 second) and accurate delivery of the gases can be performed autonomously. This gas mixture is passed through a temperature and humidity sensor prior to being delivered to the sensor array, sealed within its gas-sampling chamber. Ground truth validation access ports were incorporated at the inlet and outlet of the sensor array chamber. Table 3 lists the four mine gases along with their concentration ranges of interest. The gas delivery system is computer controlled and, once programmed, completely autonomous. The sensors array is controlled via custom measurement and control electronics, power management circuitry for sensor array and miniature diaphragm pump, and communication electronics to record and relay data to a laptop computer.
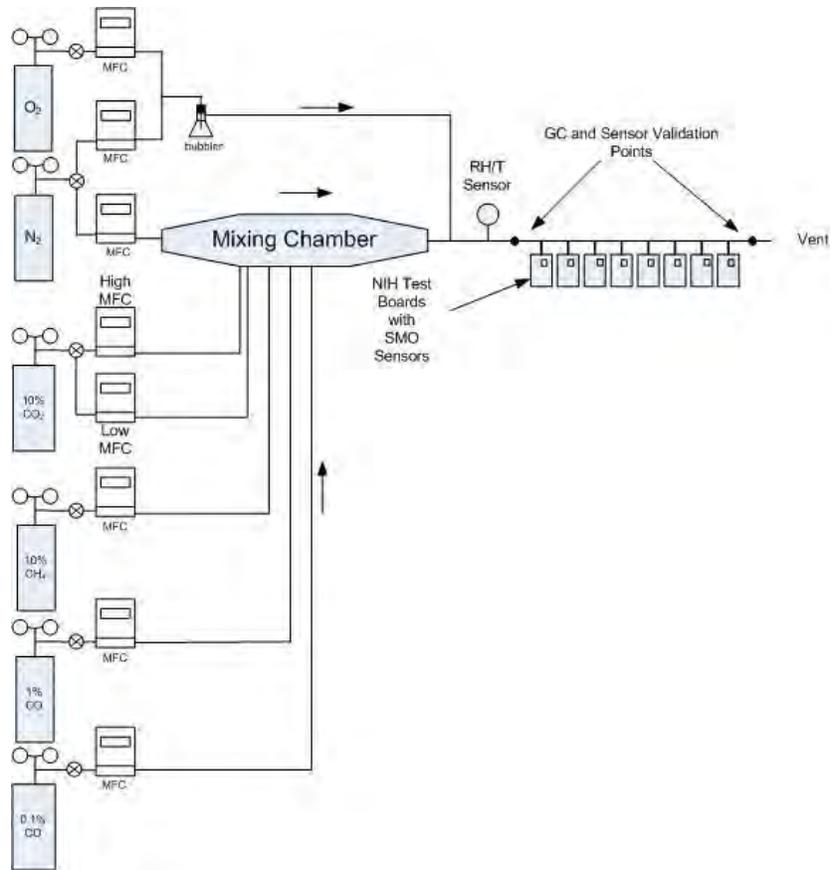
Figure 13: Schematic of gas delivery system developed to support the Phase I program.

Table 3: Mine gas concentrations used during Phase I gas testing.

Chemical Analyte	Low concentration	High concentration	Critical concentration
Methane	0.1200 ppm	1.0%	0.5% low alarm 1.0 % shut off alarm
Carbon monoxide	10 ppm	1200 ppm	35 ppm NIOSH alarm 50 ppm OSHA alarm
Carbon dioxide	0.1200 ppm	1.0%	0.5% PEL level
Oxygen	18.0%	22.0%	19.5% NIOSH low alarm

Gas Testing Protocols:

Throughout the entire Phase I program, SRD used the gas delivery system to challenge the sensor arrays to a test matrix of combustion and atmospheric gases. Due to the high humidity expected in typical coal mines, all Phase I testing was performed at room temperature and at 80% relative humidity (RH). The gas testing protocols includes the following scenarios:

1. Detection of sudden change in concentration of each of the mine gases while the concentrations of the other target gases Final testing was to repeat Table 5 test sequences a second time for the purpose of challenging the sensor array while simultaneously coupled with the signal processing algorithms to determine the overall performance metrics for detection, classification, and quantification. in the environment are maintained constant and
2. Detection of a gradual change in concentration of each target gas while the concentrations of the other target gases in the environment are maintained constant.

The first protocol is designed to test the sudden release of a gas due to the discovery of a gas pocket, while the second protocol is designed to test the more difficult and dangerous condition when there is a gradual release of gas from fissures or just from basic consumption during day-to-day mining activities. In order to serve as an early warning device for mines, the concentrations selected for testing of the gases was based on the low, high and critical gas concentrations for each of the target gases. The specific concentration ranges of interest for each mine gas is detailed in Table 3.

The initial gas testing sequences performed in Phase I focused on exposing the SMO sensor array to sudden changes in mine gas concentrations as depicted in Figure 14. Note that each mine gas has its unique gas testing protocol to properly evaluate the sensor array to critical concentrations relevant to each mine gas.
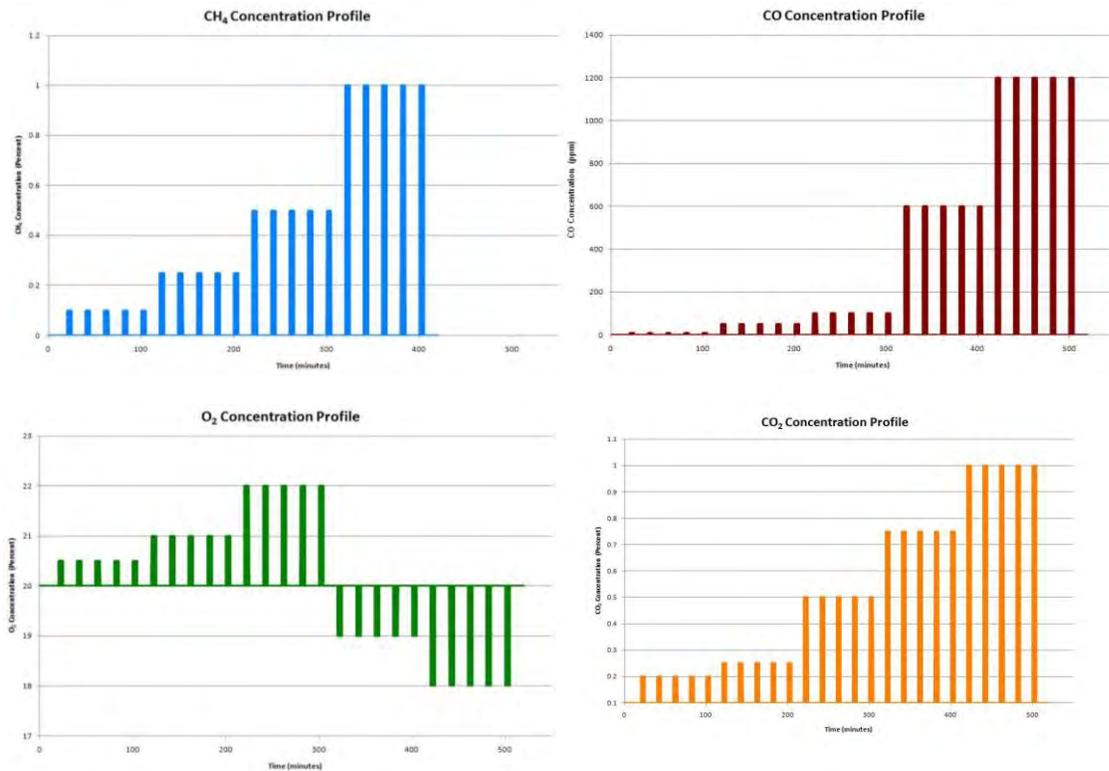

Figure 14: Gas testing protocols of all four mine gases to expose the sensor array for evaluation.

All gas test protocols delivered the baseline conditions for 20 minutes then using the autonomous gas delivery system change the gas mixture by instantaneously adding the concentration of the specific mine gas for 5 minutes before removing the mine gas and returning to the baseline conditions for another 15 minutes. This gas test cycle was replicated 5 times, for statistical purposes, at each concentration level for all four mine gases. Table 4 details the baseline parameters for each of the gas test protocols depicted in Figure 14. SRD used the Sensor Array data, collected during these tests, to evaluate the sensors individually and to feed the signal processing algorithms in Task 4.

Table 4: Description of Gas Delivery for Initial Testing of the Sensor Arrays

Chemical Run for CH4	Baseline composition
5 hits of Baseline + 0.1% CH4	80%RH/ 25 C/ 19.5% O2/ 0.1% CO2
5 hits of Baseline + 0.25% CH4	80%RH/ 25 C/ 19.5% O2/ 0.1% CO2
5 hits of Baseline + 0.5% CH4	80%RH/ 25 C/ 19.5% O2/ 0.1% CO2
5 hits of Baseline + 1.0% CH4	80%RH/ 25 C/ 19.5% O2/ 0.1% CO2
Chemical Run for CO	Baseline composition
5 hits of Baseline + 10 ppm CO	80%RH/ 25 C/ 19.5% O2/ 0.1% CO2
5 hits of Baseline + 50 ppm CO	80%RH/ 25 C/ 19.5% O2/ 0.1% CO2
5 hits of Baseline + 100 ppm CO	80%RH/ 25 C/ 19.5% O2/ 0.1% CO2
5 hits of Baseline + 600 ppm CO	80%RH/ 25 C/ 19.5% O2/ 0.1% CO2
5 hits of Baseline + 1200 ppm CO	80%RH/ 25 C/ 19.5% O2/ 0.1% CO2
Chemical Run for CO2	Baseline composition
5 hits of Baseline +0.1% CO2 (0.2% CO2)	80%RH/ 25 C/ 19.5% O2/ 0.1% CO2/ 0.1% CH4 / 10 ppm CO
5 hits of Baseline +0.15% CO2 (0.25% CO2)	80%RH/ 25 C/ 19.5% O2/ 0.1% CO2/ 0.1% CH4 / 10 ppm CO
5 hits of Baseline +0.4% CO2 (0.5% CO2)	80%RH/ 25 C/ 19.5% O2/ 0.1% CO2/ 0.1% CH4 / 10 ppm CO
5 hits of Baseline +0.65% CO2 (0.75% CO2)	80%RH/ 25 C/ 19.5% O2/ 0.1% CO2/ 0.1% CH4 / 10 ppm CO
5 hits of Baseline +0.9% CO2 (1.0% CO2)	80%RH/ 25 C/ 19.5% O2/ 0.1% CO2/ 0.1% CH4 / 10 ppm CO
Chemical Run for O2	Baseline composition
5 hits of Baseline +0.5% O2 (20.5% O2)	80%RH/ 25 C/ 20% O2/ 0.1% CO2/ 0.1% CH4 / 10 ppm CO
5 hits of Baseline + 1.0% O2 (21% O2)	80%RH/ 25 C/ 20% O2/ 0.1% CO2/ 0.1% CH4 / 10 ppm CO
5 hits of Baseline +2.0% O2 (22% O2)	80%RH/ 25 C/ 20% O2/ 0.1% CO2/ 0.1% CH4 / 10 ppm CO
5 hits of Baseline- 1.0% O2 (19% O2)	80%RH/ 25 C/ 20% O2/ 0.1% CO2/ 0.1% CH4 / 10 ppm CO
5 hits of Baseline-2.0% O2 (18% O2)	80%RH/ 25 C/ 20% O2/ 0.1% CO2/ 0.1% CH4 / 10 ppm CO

After the initial gas testing was completed, SRD subjected the sensor array to various ramp testing from either zero concentration of mine gas or lowest alarm level of mine gas to its highest concentration as described in Table 3. The rates of the changing concentrations decrease with each of the four ramp tests for each of the four mine gases as graphically represented in Figure 15.

The concentration ramp testing sequences begin with delivering baseline conditions for 20 minutes followed by the first ramp sequence, followed by another 20 minutes of baseline conditions, followed by the second ramp sequence until all ramps were performed and then finishing again with 20 minutes of baseline conditions as described in Table 5. The ramp testing evaluates the sensor array's ability to detect, identify, and quantify more realistic mine gas conditions including plumes and possibly slowly rising concentrations that would be undetected by other detectors. Final testing consisted of repeating Table 5 test sequences for a second time for the purpose of challenging the sensor array, coupled with the signal processing algorithms, to autonomously determine the overall performance metrics for detection, classification, and quantification.
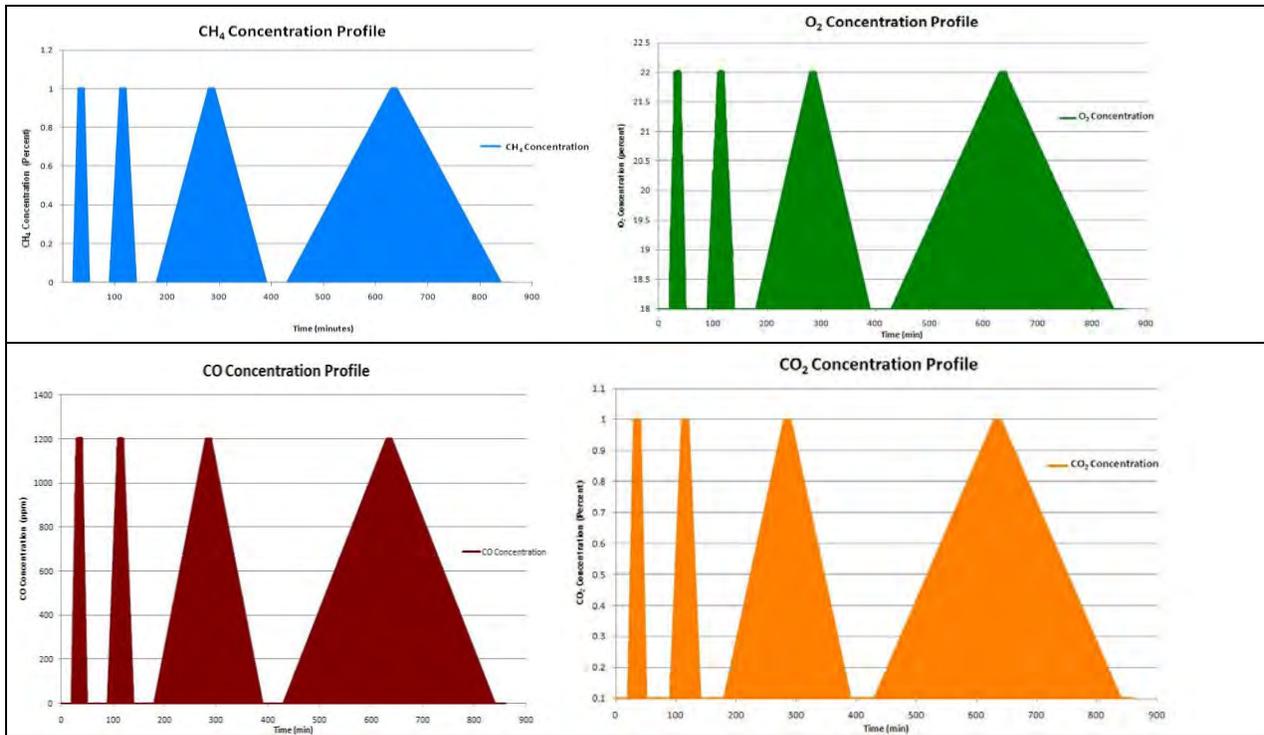
Figure 15: Four concentration profiles for mine gas ramp testing sequences

Table 5: Description of Gas Delivery for Ramp Testing of the Sensor Arrays

Ramp Testing for CH4	Baseline composition
Changing CH4 concentration from 0 to 1% to 0 at a rate of 0.1%	80%RH/ 25 C/ 19.5% O2/ 0.1% CO2
Changing CH4 concentration from 0 to 1% to 0 at a rate of 0.05%	80%RH/ 25 C/ 19.5% O2/ 0.1% CO2
Changing CH4 concentration from 0 to 1% to 0 at a rate of 0.01%	80%RH/ 25 C/ 19.5% O2/ 0.1% CO2
Changing CH4 concentration from 0 to 1% to 0 at a rate of 0.005%	80%RH/ 25 C/ 19.5% O2/ 0.1% CO2
Ramp Testing for CO	Baseline composition
Changing CO concentration from 0 to 1200ppm to 0 at a rate of 120 ppm per min	80%RH/ 25 C/ 19.5% O2/ 0.1% CO2
Changing CO concentration from 0 to 1200ppm to 0 at a rate of 60 ppm per min	80%RH/ 25 C/ 19.5% O2/ 0.1% CO2
Changing CO concentration from 0 to 1200ppm to 0 at a rate of 12 ppm per min	80%RH/ 25 C/ 19.5% O2/ 0.1% CO2
Changing CO concentration from 0 to 1200ppm to 0 at a rate of 6 ppm per min	80%RH/ 25 C/ 19.5% O2/ 0.1% CO2
Ramp Testing for O2	Baseline composition
Changing O2 concentration from 18.0% to 22.0% to 18.0% at a rate of 0.4% per min	80%RH/ 25 C/ 0.1% CO2/0.1% CH4
Changing O2 concentration from 18.0% to 22.0% to 18.0% at a rate of 0.2% per min	80%RH/ 25 C/ 0.1% CO2/0.1% CH4
Changing O2 concentration from 18.0% to 22.0% to 18.0% at a rate of 0.04% per min	80%RH/ 25 C/ 0.1% CO2/0.1% CH4
Changing O2 concentration from 18.0% to 22.0% to 18.0% at a rate of 0.02% per min	80%RH/ 25 C/ 0.1% CO2/0.1% CH4
Ramp Testing for CO2	Baseline composition
Changing CO2 concentration from 0.1% to 1% to 0.1% at a rate of 0.1%	80%RH/ 25 C/ 19.5% O2/ 0.1% CO2/0.1% CH4
Changing CO2 concentration from 0.1% to 1% to 0.1% at a rate of 0.05%	80%RH/ 25 C/ 19.5% O2/ 0.1% CO2/0.1% CH4
Changing CO2 concentration from 0.1% to 1% to 0.1% at a rate of 0.01%	80%RH/ 25 C/ 19.5% O2/ 0.1% CO2/0.1% CH4
Changing CO2 concentration from 0.1% to 1% to 0.1% at a rate of 0.005%	80%RH/ 25 C/ 19.5% O2/ 0.1% CO2/0.1% CH4

<u>Validating Gas Delivery Conditions:</u>

SRD verified the custom gas delivery system, developed to support all of Phase I testing, using certified gas cylinders and mass flow controllers as the primary method. Additionally, SRD obtained ground truth validation of each mine gas using gas chromatography coupled with a thermal conductivity detector (GC/TCD). A Restek Rt-Q-plot column was purchased for the separation and all the concentrations delivered were in the detection capability of the GC/TCD. This column was recommended to SRD by the manufacturer claiming that it was capable of separating the four gases of interest including CH_4, CO, CO_2, and O_2 at room temperature. However, this alleged separation capability was not observed in the laboratory. SRD contacted the manufacturer of the issue and was advised to lower the temperature of the chromatograph. SRD lowered the column temperature to 35 ˚C, 30 ˚C, and 25˚C (lowest temperature of GC oven) with still no separation between the mine gases. SRD attempted to separate the gases, using this same column, using their gas chromatography coupled with mass spectroscopy (GC/MS), still with no success. The carrier gas of the GC/TCD was also changed from helium to hydrogen to see if the efficiency of separation could be improved. The GC/TCD was then set up with a chiller to lower the temperature of the oven/column. The chiller was set to its lowest temperature setting which resulted in the GC/TCD being lowered to 20˚C. This resulted in methane being separated from the other three gases. The injector temperature was kept at 35˚C which is the lowest temperature on the GC/TCD. The TCD detector was kept at temperature of 200˚C and current of 75 mA for maximum sensitivity. A calibration curve established to measure methane from the gas delivery system. Figure 16 shows the TCD chromatograph for different dilutions.
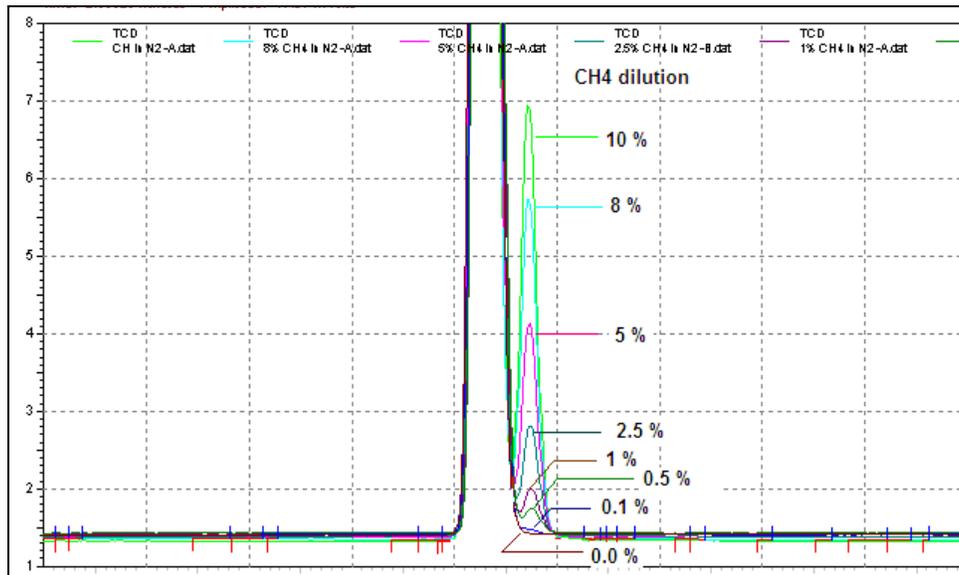

Figure 16: GC Calibration Overlay Plot for Methane Gas.

The GC/TCD was then used to verify 0.1, 0.25, 0.5, 1.0% of methane with the background gas consisting of 20.75 O_2, 0.1% CO_2, and 80 %RH. Table 6 summarizes the average ground truth validation results obtained from the GC/TCD for CH_4. Due to the lack of gas separation for CO, CO_2, and O_2, SRD was unable to acquire reliable ground truth validation measurements with the GC/TCD or GC/MS. However, SRD did use certified gas cylinders of all three gases and certified MFCs to dilute the gases to the target concentrations.

Table 6: Results of GC/TCD validation for CH$_4$ in Background gases

CH4 Target Gas in %	Average of GC/TCD Results
0	0
0.1	0.098
0.25	0.24
0.5	0.55
1	1.04

5.1.4.3 Evaluate filters and flame arrestor techniques

In the harsh conditions expected in mining environments, diesel exhaust and mining particulate matter are expected in normal operating conditions. SRD evaluated a Gore water/particulate filter along with an in-house flame arrestor to mitigate the harsh, and potentially explosive, conditions with its detector. Specifically, SRD chose a Gore filter to eliminate particulate matter to 0.2 microns and designed an in-house flame arrestor to prevent explosions from spreading upstream from the sensor. Gore was chosen because of its low chemical retention of the target gases and its ability to restrict liquid water (not vapors) from entering the gas sampling system to the sensor array.   SRD designed and constructed a Teflon housing, as shown in Figure 17, to integrate and test the Gore filter as an addition to the gas-sampling system as shown in Figure 19.
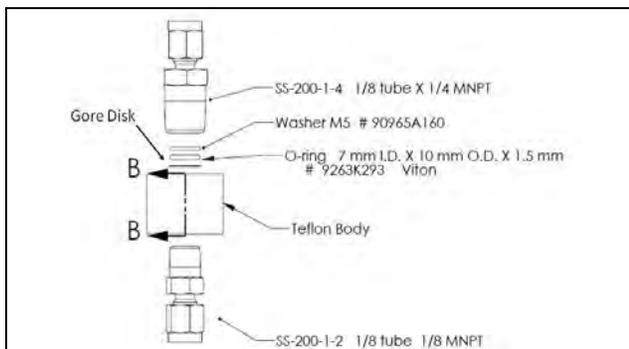

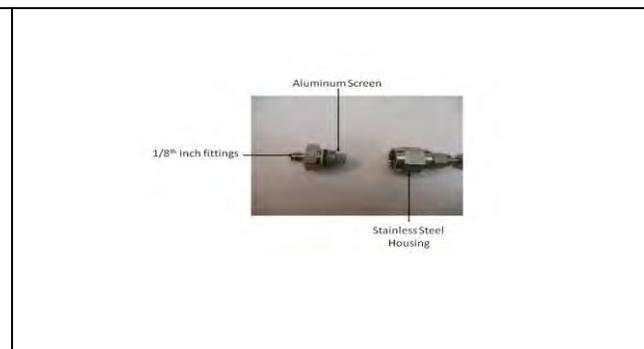**Figure 17: Gore Filter Assembly Used in Phase I Testing.**

Figure 18: SRD's in-house fixture flame arrestor.

Finding a flame arrestor for SRD's low volume, low flow rate and small size restriction was unsuccessful. The smallest flame arrestor found was for a 3/8th welding torch that wasn't rated for methane. The next size up was over 1 inch pipe fittings. SRD decided to make an in-house flame arrestor. The housing of a 1/8 inch 1/3 lb Swagelok check valve was used with a piece of 120 X120 X 0.0036 Aluminum mesh cut to 0.6 wide X 10 inches long which is 30.7% open. A photograph of the in-house flame arrestor is shown in Figure 18.

The flame arrestor was assembled and tested to evaluate its capability to arrest flames. A 1 liter Tedlar bag of the flammable gas of 10 % CH$_4$ in 20 % O$_2$ (LEL 5.1%) was filled. The flame arrestor described above was placed in-line with the Tedlar bag and gas was flowed through the flame arrestor to an ignition source (gas lighter). After approximately 200 mL of gas was passed

through the filter the gas was ignited at the end of the tube. The flame never made it past the in-house flame arrestor and to the Tedlar bag. This was repeated 5 times and then also repeated with 15% H_2 in 20% O_2. This in-house flame arrestor was then placed in series with the Gore filter previously described and placed on the in-house gas delivery system as shown in Figure 19.

Figure 19: Gore Filter and Flame Arrestor in sequence on Gas Delivery System prior to Sensor Array

The Sensor Array was subjected to 5 hits of 0.5% of CH_4, 5 hits of 600ppm CO, 5 hits of 22% O_2 and 5 hits of 18% O_2 both with and without the gore filter and flame arrestor to determine if they altered the Sensor Array's response by altering which gases reach the sensors and at what concentrations. Figure 20 compares the sensors' responses to the four mine gases both with and without the gore filter and flame arrestor inline. As can be seen from the four sensor response plots, the presence of the gore filter and flame arrestor **do not** change the sensor responses to the four gases. The solid blue line represents the sensors' responses with filters present, while the solid green line represents the same sensors' responses without the filters. The error bars indicate the spread of responses over the five replicate trials. As can be seen the response magnitudes are well within the error bars indicating no effect of filters on sensor response characteristics.
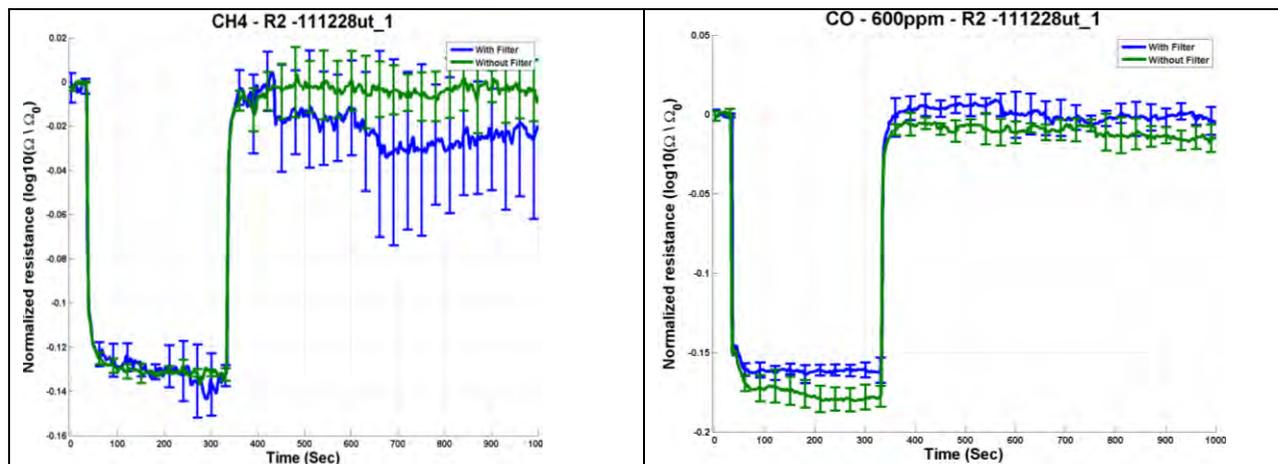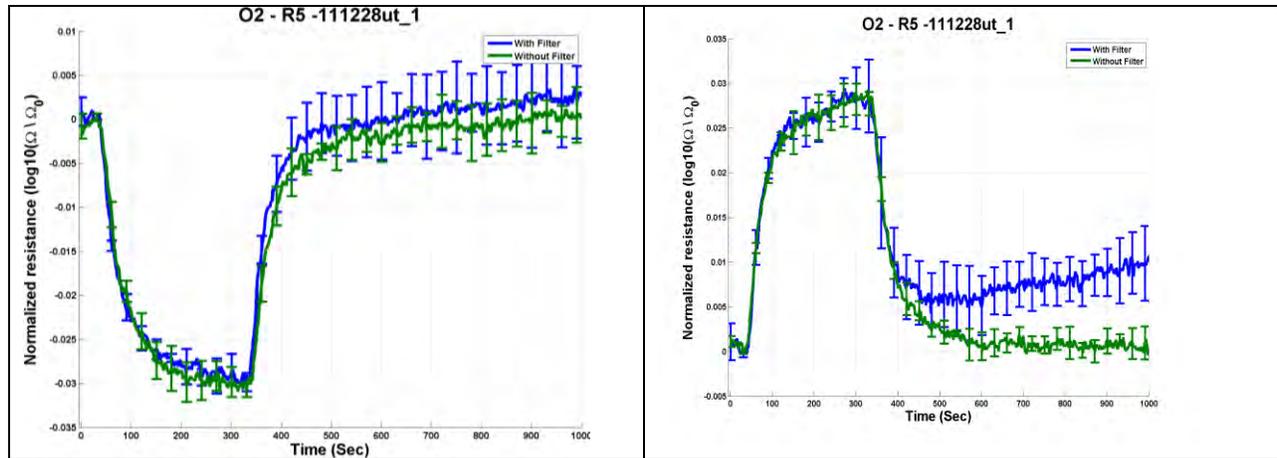
Figure 20: Comparison of sensor responses with and without filters to 0.5% of CH4 (top left), 600 ppm of CO (top right), 18% O2 (bottom left) and 22% O2 (bottom right).

5.1.4.4 Develop sensor array signal processing algorithms

SRD implemented a hierarchical approach to detect, identify and quantify the mine gases present in the environment. The data is continuously processed by the hit-detection algorithm whose function is to monitor if any threats are encountered (i.e. target gases are present). If the algorithm detects an event, it extracts key features of the response and invokes the classification algorithm. The classification algorithm is the second stage of the process. Its main job is to identify an event whenever called into action by the hit-detection algorithm. Once the classification algorithm identifies the gas, it invokes the quantitation algorithm. The quantitation algorithm takes the output of the hit-detection algorithm (key features of response) and classification algorithm (identity of gas), uses this information to provide estimates of the concentration of gas. Once its task is completed, control is handed back to the hit-detection algorithm (which has been running in the background). This occurs on a sample-to-sample basis until the hit-detection algorithm determines that the threat is completely removed.
A more detailed discussion of the three-stage algorithm architecture is provided in the following subsections.

In order for the hit detection algorithm to detect the mining gases including methane, carbon monoxide, oxygen, and carbon dioxide, the algorithm's statistical parameters and its logic will require refinement. The statistical information obtained from exposing the selected sensor array to target gases was used in Phase I for refining the algorithm. In particular, information such as rates of sensor responses, recoveries, response magnitudes, and baseline behavior was used for refining the hit detection algorithm.

SRD uses feature extraction and pattern recognition methods such as Neural Networks, Support Vector Machine, and Curve fitting methods for the identification and quantitation of target gases. Following the detection of a gas, SRD's architecture uses the above methods to identify the gas and determine the gas concentration. The use of multiple algorithms allows the architecture to become robust and maintain a low (below 1%) false alarm rate. The results from individual algorithms are combined via a data fusion algorithm to provide a single, robust output.

In Phase I, a training database was established for identification and quantitation of the four mining gases. These databases consist of a library of known sensor response characteristics to the target gases at given concentration levels. The pattern recognition algorithms query these databases in the event a hit (presence of a gas) is determined. SRD uses the information from exposing the selected sensor array to target gases for establishing the databases. The information includes pattern recognition parameters, feature extraction values of sensor response magnitudes, corresponding gas indices, and corresponding gas concentration values.

"Raw" Sensor Response Signals:

This section provides the "raw" sensor response signals for each sensor that targets each of the four mine gases. Each sensor's responses, for each concentration level, are plotted together to demonstrate the quantitative information within the sensor response signals.

METHANE:

Table 7 summarizes the gas testing protocol for detecting sudden changes in methane when the background constituents of oxygen and carbon dioxide are kept constant. The protocol for testing is illustrated in Figure 14 in the previous section. The sensor array was exposed to increasing levels of methane (0.1200 ppm, 0.25%, 0.5% and 1200 ppm) while keeping the background composition of 20.75% oxygen, 0.1200 ppm CO_2. Testing was performed at 80% RH and 25°C. Figure 21 compares the response of sensors 2 and 4 to the different levels of methane. The spread of responses to the different concentrations of methane demonstrates that the sensors are capable of providing concentration estimates for methane. Table 8 below shows the relative standard deviation (RSD) across the trials for each concentration of methane gas exposure for sensor materials 2 and 4. The average relative standard deviation (RSD) is 2.43% for sensor 2 and 2.5% for sensor 4. The low RSD values indicate accurate gas delivery over different trials of same concentration and good sensor response repeatability, indicating high precision.

Table 7: Testing protocol for methane (CH$_4$).

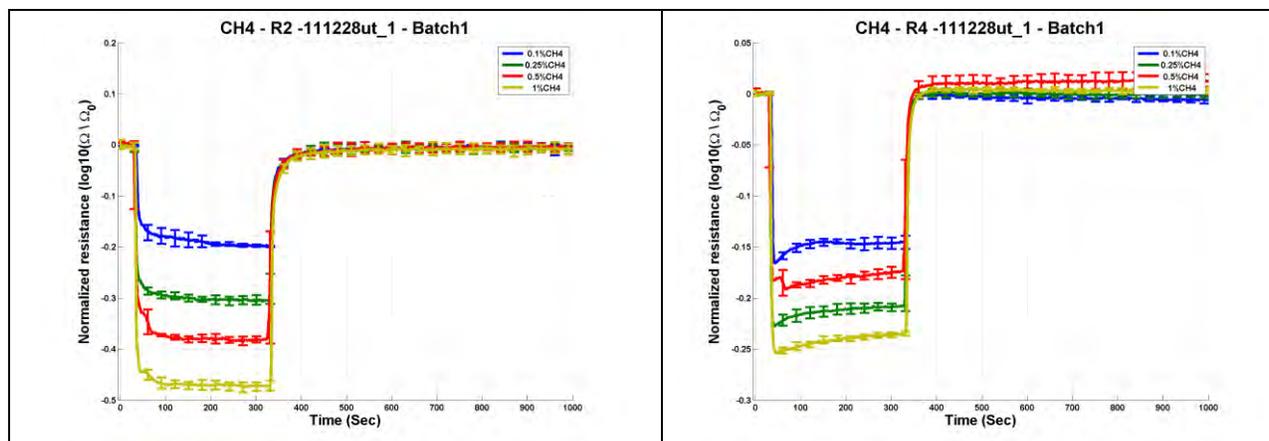| CH4		
Test #	**Chemical Run**	**Baseline composition**
1	5 hits of Baseline + 0.1200 ppm CH4	80%RH/ 25 C/ 19.5% O2/ 0.1200 ppm CO2
2	5 hits of Baseline + 0.25% CH4	80%RH/ 25 C/ 19.5% O2/ 0.1200 ppm CO2
3	5 hits of Baseline + 0.5% CH4	80%RH/ 25 C/ 19.5% O2/ 0.1200 ppm CO2
4	5 hits of Baseline + 1.0% CH4	80%RH/ 25 C/ 19.5% O2/ 0.1200 ppm CO2

Figure 21: Response of sensors 2 and 4 to varying concentrations of CH4 for eight different chips.

Table 8: Percentage relative standard deviation across trials for different concentrations of Methane (CH$_4$).

% RSD for different concentrations of CH$_4$				
Sensor/Conc	0.10%	0.25%	0.50%	1.00%
2	0.39	2.51	4.85	2.00
4	3.60	1.81	3.87	0.74

CARBON MONOXIDE:

Table 9 shows the CO testing protocol for detecting sudden changes in CO when the background constituents of oxygen and carbon dioxide are kept constant. The CO testing protocol is illustrated in Figure 14 in the preceding section. As indicated in Table 9, the sensor array was exposed to increasing levels of carbon monoxide (10 ppm, 50 ppm, 100 ppm, 600 ppm and 1200 ppm) while keeping the background composition of 20.75% oxygen, 0.1200 ppm CO2 constant. Testing was performed at 80% RH and 25°C. Figure 22 compares the responses of sensors 1 and 2 to the different concentration levels of CO. The spread of responses to the different CO concentrations demonstrates that the sensors are capable of providing good CO concentration estimates. Table 10 summarizes the RSDs across the trials for each of the CO concentration exposures for sensors 1 and 2. The average RSD is 30.73% for sensor 1 and 2.56% for sensor 2. The average RSD value for sensor 1 is skewed due to the larger variation at the lower concentration of 10 ppm. However, since the RSD of sensor 2 is much better, use of sensor 2 will be made to estimate concentrations of CO. Sensor 1 will be used as a backup sensor to sensor 2 to provide robustness to the system in the event of failure of sensor 2.

Table 9: Testing protocol for carbon monoxide (CO).

CO		
Test #	Chemical Run	Baseline composition
1	5 hits of Baseline + 10 ppm CO	80%RH/ 25 C/ 20.75% O2/ 0.1200 ppm CO2

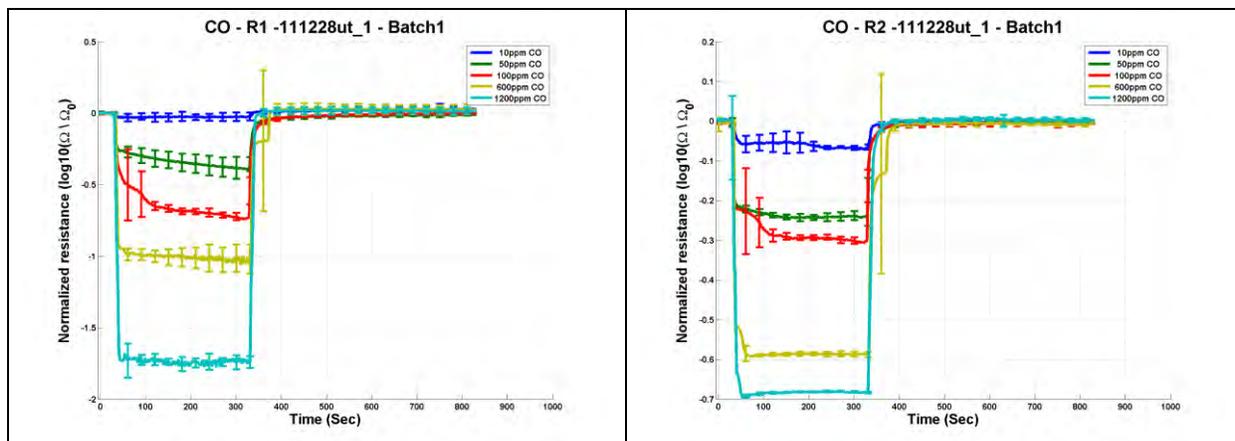|		
2	5 hits of Baseline + 50 ppm CO	80%RH/ 25 C/ 20.75% O2/ 0.1200 ppm CO2
3	5 hits of Baseline + 100 ppm CO	80%RH/ 25 C/ 20.75% O2/ 0.1200 ppm CO2
4	5 hits of Baseline + 600 ppm CO	80%RH/ 25 C/ 20.75% O2/ 0.1200 ppm CO2
5	5 hits of Baseline + 1200 ppm CO	80%RH/ 25 C/ 20.75% O2/ 0.1200 ppm CO2

Figure 22: Response of sensors 1 and 2 to varying concentrations of CO for eight different sensor arrays.

Table 10: Percentage relative standard deviation across trials for different concentrations of CO.

% RSD for different concentrations of CO					
Sensor/Conc	**10 ppm**	**50 ppm**	**100 ppm**	**600 ppm**	**1200 ppm**
1	122.18	18.11	2.96	8.49	1.91
2	4.06	3.86	3.50	1.03	0.36

OXYGEN:

Table 11 provides the testing protocol for detecting sudden changes in O_2 levels when the background constituents of CO and CO_2 are kept constant. The sensor array was exposed to different levels of oxygen (20.5%, 21200 ppm, 22%, 19%, and 18%) while keeping the background composition of 20% O_2, 10ppm CO_2 and 0.1200 ppm CO constant. Testing was performed at 80% RH and 25°C. The concentrations of O_2 were changed by 0.5%, 1200 ppm, 2%, -1200 ppm and -2% relative to the background composition of O_2. Figure 23 shows the response of sensors 4 and 5 to the different levels of O_2. It should be noted that some responses go up while other have a downward response. This is because the testing is conducted around the baseline levels of O_2 with some of the O_2 concentrations increase above the baseline value while others decrease below the baseline value. Table 12 summarizes the RSD across the trials for

each concentration of oxygen gas exposure for sensor materials 4 and 5. The average RSD is 21.57% for sensor 4 and 15.57% for sensor 5. With Sensor 5's lower RSD, it will be used to estimate O_2 levels. Sensor 4 will be used as a backup sensor to sensor 5 to provide robustness to the system in the event of failure of sensor 5.

Table 11: Testing protocol for oxygen (O_2).

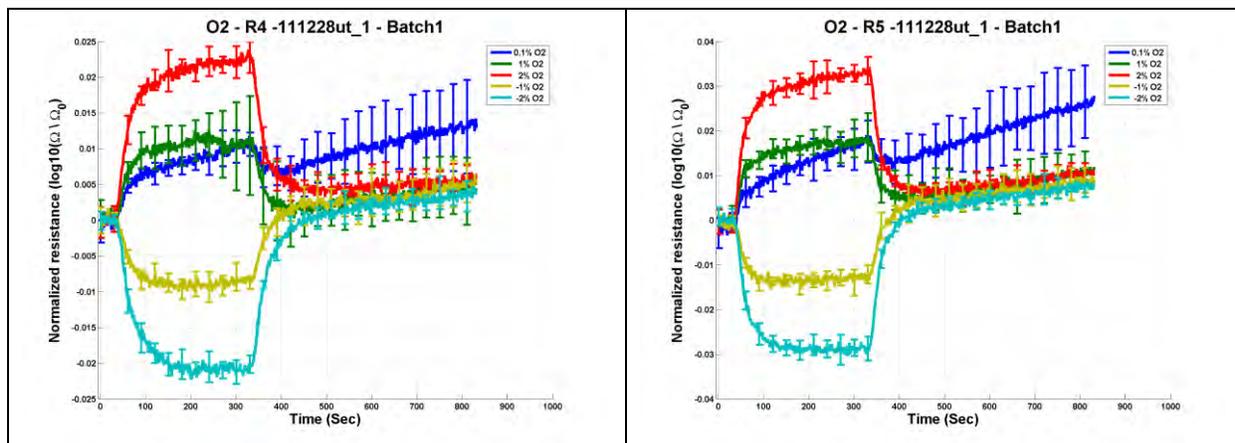| CO		
Test #	Chemical Run	Baseline composition
1	5 hits of Baseline + 20.5% O_2	80%RH/ 25 C/ 20.5% O_2/0.1200 ppm CO2/ 10ppm CO
2	5 hits of Baseline + 21200 ppm O_2	80%RH/ 25 C/ 20.5% O_2/0.1200 ppm CO2/ 10ppm CO
3	5 hits of Baseline + 22% O_2	80%RH/ 25 C/ 20.5% O_2/0.1200 ppm CO2/ 10ppm CO
4	5 hits of Baseline + 19% O_2	80%RH/ 25 C/ 20.5% O_2/0.1200 ppm CO2/ 10ppm CO
5	5 hits of Baseline + 18% O_2	80%RH/ 25 C/ 20.5% O_2/0.1200 ppm CO2/ 10ppm CO

Figure 23: Response of sensors 4 and 5 to varying concentrations of O2 for eight different chips.

Table 12: Percentage relative standard deviation across trials for different concentrations of oxygen.

% RSD for different concentrations of O2					
Sensor/Conc	20.50%	21.00%	22.00%	19.00%	18%
4	19.59	55.63	6.56	20.72	5.36
5	27.48	24.67	7.38	12.85	5.46

CARBON DIOXIDE:

Table 13 summarizes the testing protocol for detecting sudden changes in CO_2 when the background constituents of CO, CH_4 and O_2 are kept constant. The protocol for testing is illustrated in Figure 14 in the preceding section. The sensor array was exposed to different CO_2 levels (0.1200 ppm, 0.15%, 0.4%, 0.65% and 0.9%) while keeping the background composition of 20.75% O_2, 0.1200 ppm ppm CO_2 , 10ppm CO and 0.1200 ppm CH_4 constant. Testing was performed at 80% RH and 25°C. Figure 24 compares the responses of sensors 4 and 5 to the different levels of CO_2. The result for the lowest concentration of CO_2 is skewed. However, the median RSD is 25.34% for sensor 1. SRD will improve upon the RSD for the CO_2 sensor as part of the Phase II work. This may involve testing additional materials and/or implementing rigid quality control measures during development of the CO_2 sensors.

Table 13: Testing protocol for carbon dioxide (CO_2).

| CO_2		
Test #	Chemical Run	Baseline composition
1	5 hits of Baseline + 0.2% CO_2	80%RH/ 25 C/ 20.75% O_2/0.1200 ppm CO2/ 10ppm CO/0.1200 ppm CH_4
2	5 hits of Baseline + 0.25% CO_2	80%RH/ 25 C/ 20.75% O_2/0.1200 ppm CO2/ 10ppm CO/0.1200 ppm CH_4
3	5 hits of Baseline + 0.5% CO_2	80%RH/ 25 C/ 20.75% O_2/0.1200 ppm CO2/ 10ppm CO/0.1200 ppm CH_4
4	5 hits of Baseline + 0.75% CO_2	80%RH/ 25 C/ 20.75% O_2/0.1200 ppm CO2/ 10ppm CO/0.1200 ppm CH_4
5	5 hits of Baseline + 1.0% CO_2	80%RH/ 25 C/ 20.75% O_2/0.1200 ppm CO2/ 10ppm CO/0.1200 ppm CH_4
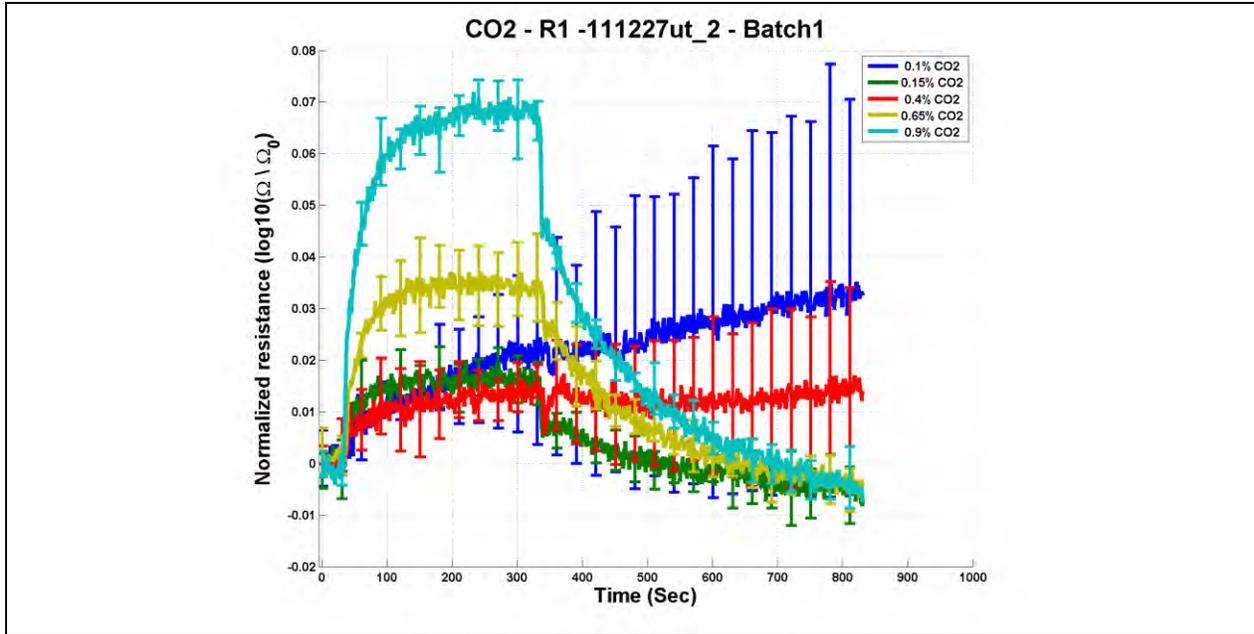
Figure 24: Response of sensor 1 to CO_2 at varying concentrations for eight different chips.

Table 14: Percentage relative standard deviation for different concentrations of CO2.

% RSD for different concentrations of CO_2				
Sensor/Conc	**0.20%**	**0.25%**	**0.50%**	**0.75%**	**1200 ppm**
1	72.35	25.34	26.21	24.02	9.02

Gas Detection:

Hit detection is the process of determining the sensor array response characteristics that refers to the presence of an actual target gas versus background conditions. SRD employs a weighted threshold detection algorithm with an adaptive baseline modeling to enable detection of sensors responses that deviate from baseline. Additionally, in order to improve the robustness of the detection algorithm, the following criteria are also used:

1. Time-based criteria to ascertain that the response deviation is due to gas and not noise,
2. Multiple sensor responses to ascertain that responses are not due to single sensor malfunction,
3. Humidity data check in order to ascertain response is not tracking humidity fluctuations,
4. Temperature data check to ascertain response is not tracking temperature fluctuations.

The hit-detection algorithm also performs the crucial role of extracting key features of the sensor response kinetics, such as magnitude deviation above threshold and slope of magnitude responses to pass onto the classification algorithm. The hit-detection algorithm also monitors for the time when the sensor array's response magnitudes return back to baseline or "non-threat", thus indicating the end of the target gas exposure.

Gas Identification:

Identification or classification is the process of identifying a target gas present in an exposure based on previously trained sensor responses to known threats. In the hierarchical approach employed, classification of a gas, once a hit has been detected, follows hit detection. The input to the classification algorithm is the output results from the hit detection algorithm (i.e. the key features of the sensor array response kinetics). SRD uses the support vector machine (SVM) classifier to identify the gas detected. More specifically, the radial basis function (RBF) kernel is used for the classifier. Prior to testing the efficiency of the classifier, the classifier needs to be trained on the key features of the sensor response kinetics using apriori information regarding the identity of the gas. This one-to-one correlation between the response kinetics and the identity of the gas aids the classifier to correctly form mathematical relations categorizing the multidimensional boundaries within which each gas response resides. It should be noted that the training is done only once offline based on an established training database.

During the real-time evaluation of the performance of the algorithm, the classifier utilizes the established relationship between responses and gases to correctly classify the unknown response that is fed to the classification algorithm. Out of the five trials (at each concentration) discussed in preceding sections, three trials were used as training data for classifier and the other two additional trials were used as blind test cases to evaluate the performance of the classifier.

Gas Quantification:

SRD's quantitation algorithm is the third and final stage in the hierarchical algorithm structure. This algorithm takes that output of the previous two stages (hit-detection and classification) to provide information on the quantity of the target gas exposed to the array. In order to provide an estimate of the concentration based on the response magnitude, a relationship between the magnitude response and concentration is required. To establish this relationship (henceforth termed calibration curve), one of the tests conducted with the gradual ramp of the target gas concentration over time was used i.e. for the concentration profile used in the ramp testing, a one-to-one relationship to the magnitude response of the sensor was obtained using cubic polynomial interpolation. Figure 25 presents the calibration curve for methane. Figure 26 shows the calibration curve for carbon monoxide. Figure 27 provides the calibration curve for oxygen.
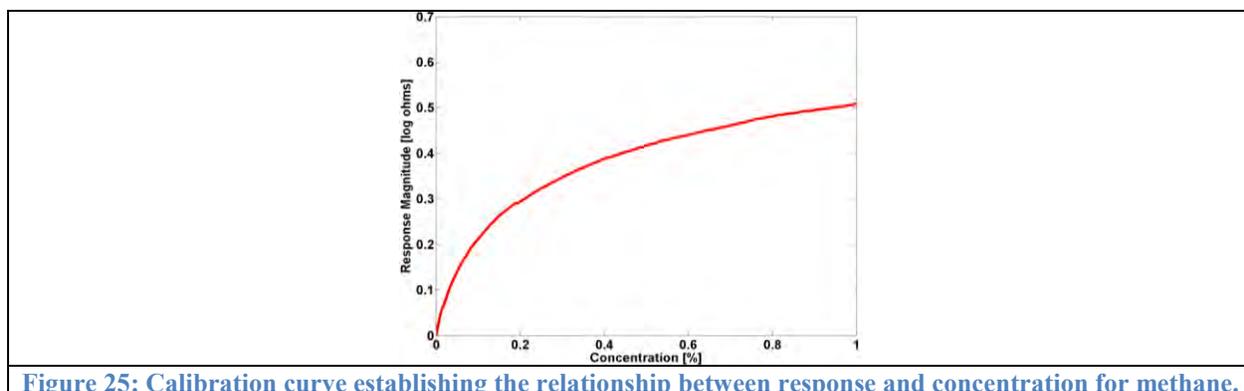

Figure 25: Calibration curve establishing the relationship between response and concentration for methane.
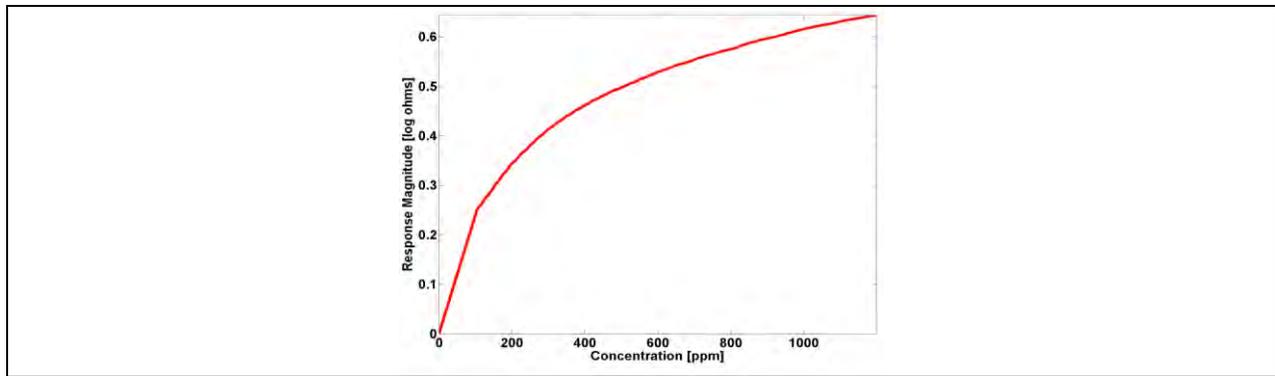
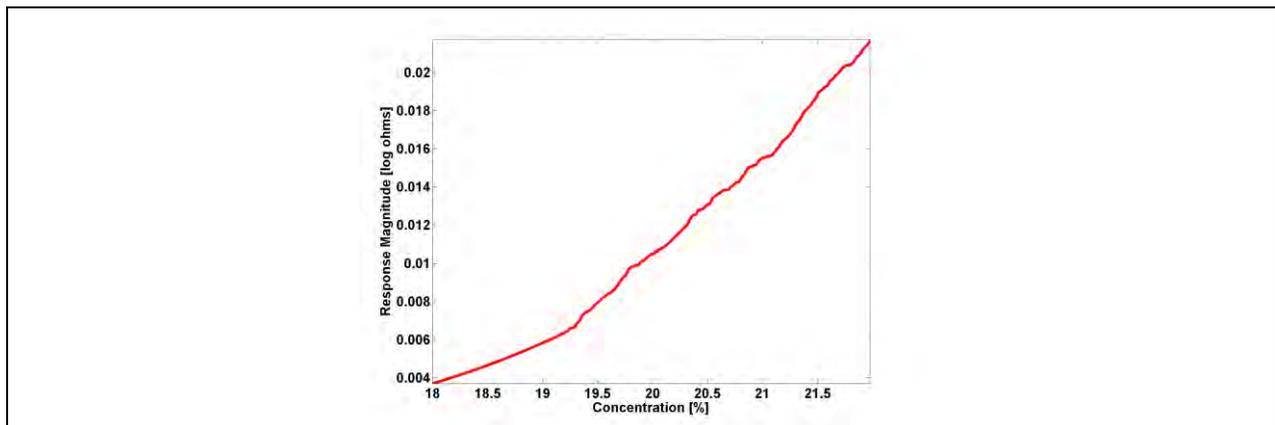**Figure 26: Calibration curve establishing the relationship between response and concentration for CO.**

Figure 27: Calibration curve establishing the relationship between response and concentration for O$_2$.

5.1.4.5 Establish the basis for a wireless sensor network (WSN)

There are currently a number of communication and tracking systems approved by MSHA to work within mines. The type of transmission used in these systems, in most cases, is split between hardwired and wireless networks. The most common hardwired system used is the "Leaky Feeder" system. This system has been the primary communication system in mines for a number of years. Although a proven technology, the limitations of this system are:

- High installation and maintenance cost
- As mines are extended, the Leaky Feeder cable and supporting hardware is not always installed until much later due to installation issues
- Cave-ins will likely cause disruption of Leaky Feeder cable service to critical areas

To help alleviate most of these limitations, numerous manufacturers continue to develop communication systems that rely totally on wireless technologies that are networked together into a meshed topology.

Mesh network operation

Mesh networking is a powerful way to route data. Range is extended by allowing data to hop node to node, and reliability is increased by the ability of the network to create alternate paths when one node fails or connection is lost. This can be especially valuable for mining applications where cave-ins can cause disruptions and damage to communications systems in areas of the mine. A mesh network of wireless sensors allows each sensor to not only capture and process sensor data, but act as a relay for other sensors to transmit data back to the base station, therefore providing a robust and self-healing system that automatically re-routes around a node that drops out due to loss of signal, operation or performance.

Wireless module selection

Reviewing previous tests of tracking and communications systems reported by the Mine Safety and Health Administration, and commercial products already with MSHA approval, there are several wireless options available for SRD to adopt to allow for a wireless sensor network. The transmission frequencies of 900MHz and 2.4GHz were selected based on their

1. Past success in underground communications systems,
2. Performance during low power consumption, and
3. Availability of off-the-shelf wireless transceivers in this frequency band.

The specific modules were selected based on their portability, ease of development, and the availability of wireless mesh network software stacks for easy multi-nodal implementation. The Atmel Atmega128 is an IEEE 802.15.4 compliant single chip that combines an AVR microcontroller and 2.4GHz RF transceiver. The device features wake-on radio, 32-bit MAC symbol counter, temperature sensor, automatic transmission modes, 128-bit AES crypto engine, true random number generator, high data rate modes, and antenna diversity support. The development kit (Figure 28) allows for easy implementation of a Zigbee wireless mesh network, and battery operation for mobile testing.

Figure 28: Atmel Atmega128RFA1 Development Board

The Digi 9XTend RF Module (Figure 29) operates within the ISM 900 MHz frequency band and sustains up to 115.2Kbps data throughput. The modules feature DigiMesh mesh networking support, and allows the user to select a transmit power from 1mWatt to 1Watt. The transceiver has a sensitivity of -100dBm.

Figure 29: Digi 9XTend 900MHz Module

The transmission frequency of 315MHz was evaluated and was determined not to be a feasible option for this project due to unavailability of off the shelf RF modules for data transfer in this frequency range, and the unavailability of a multi-nodal mesh communications protocol for this frequency band. Table 15summarizes the wireless module properties for 2.4 GHz and 900 MHz. These two wireless modules were fully evaluated in Phase I with the results presented in this section.

Table 15: Wireless Module Properties

	AVR 2.4GHz	Digi Xtend 900MHz
Rx Sensitivity	-100dBm	-100dBm
Tx Power	3.5dBm	0dBm to 30dBm
Mesh Protocol	Zigbee	DigiMesh
Antenna	2.1dBi dipole	2.1dBi dipole

Calculations

A link budget analysis can mathematically predict the system range based on the power output, receiver sensitivity, antenna gains, path loss, and fading margin. The path loss equation represents path loss (signal attenuation) as a function of distance between the receiver and transmitter and the wavelength of the operating frequency. This equation is derived from the Friis transmission equation and is given by:

Path Loss = $20 * \log(4*\pi*r/\lambda)$ dB (Eq. 1), where

r = distance between transmitter and receiver
λ = wavelength

The Friis transmission equation can be used to represent the path loss as the sum of the other system factors leading to the following equation:

Path Loss = P(t) + G(t) + G(r) - R(s) - F(s) dB (Eq. 2), where

P(t) = transmitted power
G(t) = gain of transmit antenna
G(r) = gain of receive antenna
R(s) = sensitivity of receiver
F(s) = fading margin, (experimentally determined to be 22dBm by the manufacturer)

Applying these equations for both transceivers that SRD tested:

Atmel 2.4GHz Module – 3.5dBm transmit power
$\Lambda = 0.125$ meters
(Eq. 1) Path Loss = 85.5 dB = $20 * \log(4*\pi*r/\lambda)$
(Eq. 2) Link Budget = 3.5dBm + 2dB + 2dB - (-100dBm) - 22dBm = 85.5 dB
Solving these two equations gives us a projected system range:
r = 176 meters
Digi Xtend 900 MHz Module – 0dBm transmit power
$\lambda = 0.33$ meters

(Eq. 1) Path Loss = 82 dB = 20 * log(4*π*r/λ)
(Eq. 2) Link Budget = 0dBm + 2dB + 2dB - (-100dBm) - 22dBm = 82 dB
Solving these two equations gives us a projected system range:
 r = 334m

Digi Xtend 900 MHz Module – 10dBm transmit power
λ = 0.33 meters
(Eq. 1) Path Loss = 92 dB = 20 * log(4*π*r/λ)
(Eq. 2) Link Budget = 10dBm + 2dB + 2dB - (-100dBm) - 22dBm = 92 dB
 r = 1045m

Line-of-Sight Range Test

This test is conducted in an open field (Figure 30). It begins with the transmission of 35 bytes of data from a base station transmitter to a mobile battery operated transmitter at some distance away. A successful transmission will end with a reply from the mobile transmitter received at the base station. If at any time the signal was lost, the mobile crew would move back towards the base station until communications were reestablished. Maximum range was recorded as the distance associated with the point at which only 50/100 packets were being received. The 900MHz module was tested at two Transmission power settings, 0dBm and 10dBm.
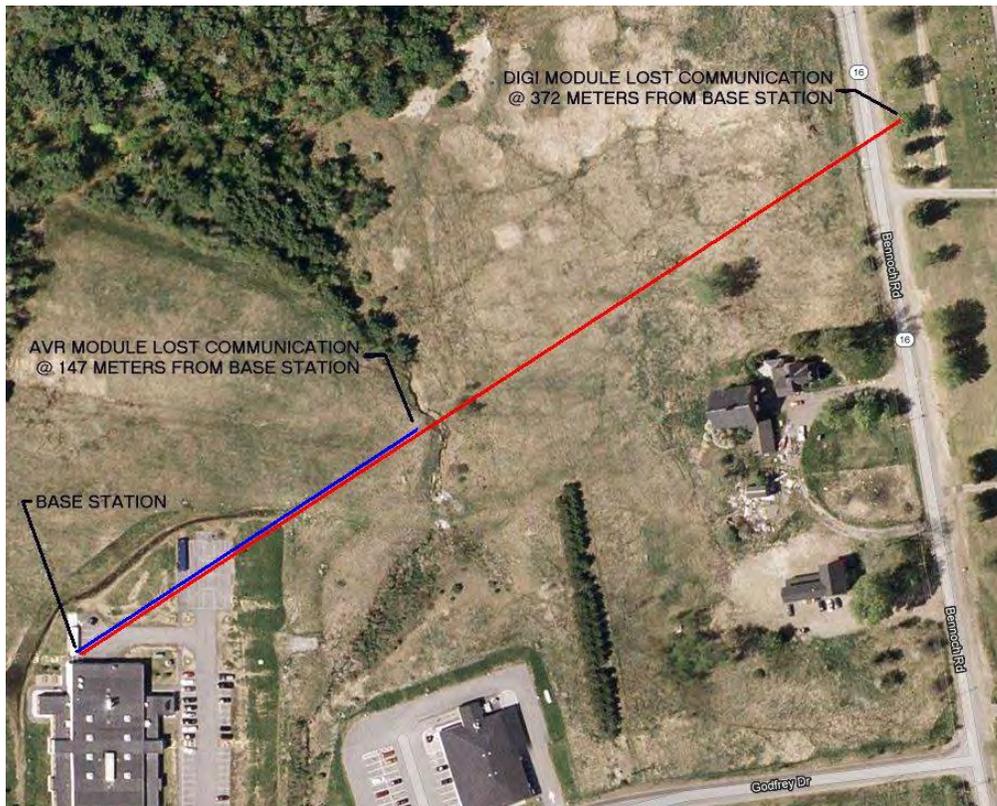

Figure 30: Line-of-Sight Range Test Site

The line-of-sight range testing is summarized in Figure 31 by comparing to the theoretical calculated range with the actual range. The 2.4GHz module lost communication with the base station and reached its maximum range at 147 meters from the base station. The 900MHz Digi module lost communication with the base station and reached its maximum range at a distance of 372 meters from the base station. When the Digi Module's transmit power was increased to 10dBm, the module's maximum range was increased to 680 meters.
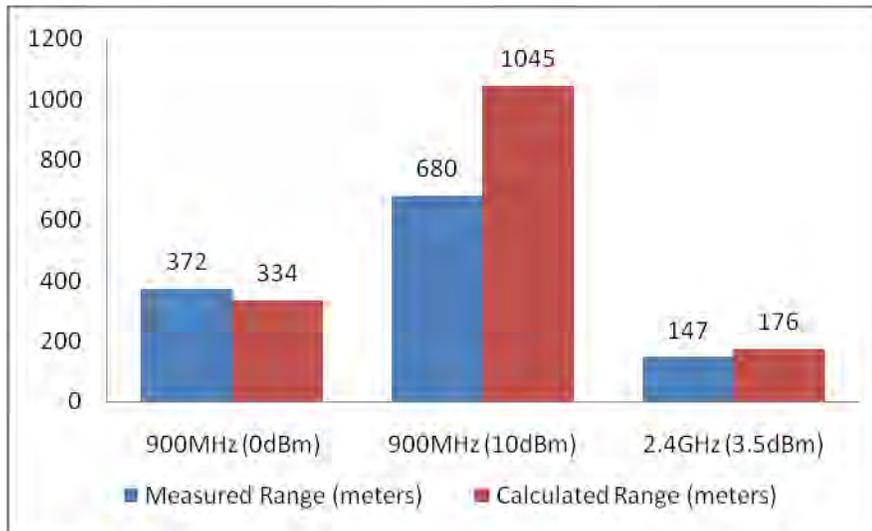

Figure 31: Line-of-Sight Range Measurements vs. Calculations

Indoor Range Test

To determine indoor range, both modules were tested inside a metal-framed building, at multiple distances between the base station and the mobile transmitter. Table 16 provides descriptions for the 6 test points inside the building along with the percentage of Packets that were received from the mobile transmitter. The Digi 900MHz module was set to 0dBm TX power.

Table 16: Summary of Six Indoor Tests to Determine Range.

distance (m)	walls	900MHz (0dBm)	2.4GHz	99MHz (10dBm)
3	0	100.0%	100.0%	100.0%
50	1	100.0%	100.0%	100.0%
70	3	100.0%	100.0%	100.0%
100	5	100.0%	99.8%	100.0%
120	5	100.0%	99.1%	100.0%
140	6	96.0%	4.7%	99.1%
170	6	59.5%	0.0%	97.5%
200	7	9.3%	0.0%	86.5%
220	7	0.0%	0.0%	55.7%
250	8	0.0%	0.0%	12.1%

The results of this test indicate that the 2.4GHz module can reliably relay data to the base station at a maximum distance of 120 feet away with 5 walls separating them, while the 900MHz Digi module can communicate reliably up to 170 feet away through 6 walls. Increasing the Digi 900MHz module's transmit power to 10dBm increases the range to 220 feet. Even at the lower power setting, the 900MHz module has greater indoor range than the 2.4GHz transceiver (Figure 32).
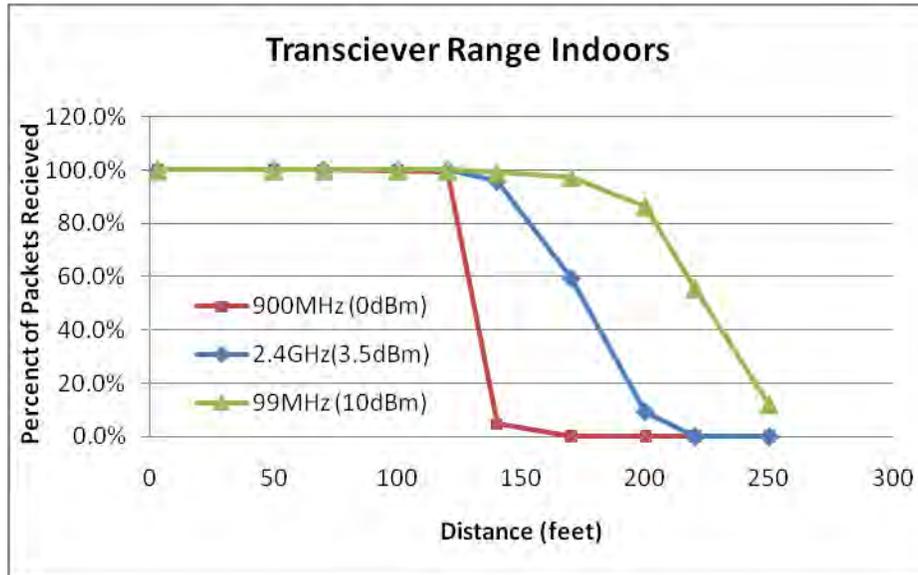

Figure 32: Graph of Indoor Range Results

Wooded Area Range Test

To determine the performance of the transceivers in an environment with no direct line-of-sight, both modules were tested inside in a wooded area with dense foliage separating the base station and the mobile transmitter. The mobile transceiver was moved further into the woods increasing separation from the base station. The results of this test show that the 2.4GHz module can reliably relay data to the base station at a maximum distance of 200 feet, while the 900MHz Digi module can communicate reliably up to 280 feet. Increasing the Digi 900MHz module's transmit power to 10dBm increases the range to 370 feet. Even at the lower power setting, the 900MHz module has greater range in a wooded area than the 2.4GHz transceiver. See Figure 33 for details.
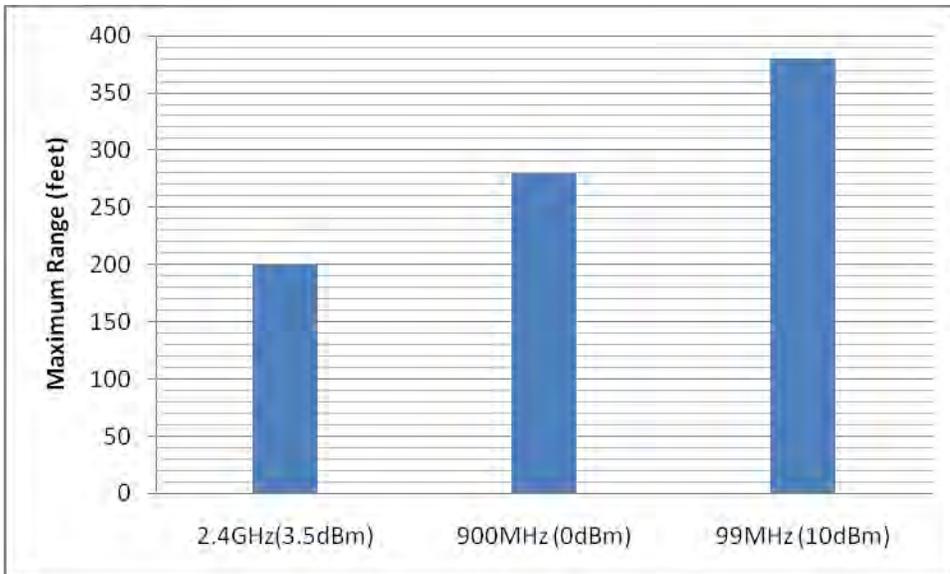
Figure 33: Maximum Range Measured in a Wooded Area

Multi-Nodal Testing

The 900 MHz Digi 9Xtend module demonstrated superior performance in each of the range testing sections when compared with the AVR 2.4GHz module. Even with a lower transmit power, the 900MHz module had a higher maximum range in all three test conditions: outdoor line-of-sight, inside a metal frames building, and in a wooded area. In this section, SRD focuses on the 900MHz Digi Xtend module's performance when configured in a multi-nodal mesh network.

Digi XTend RF Modules feature DigiMesh™ mesh net-working support. Mesh networking allows messages to be routed through several different nodes to a final destination. The DigiMesh firmware allows system integrators to bolster their networks with the self-healing attributes of mesh networking. In the event that one RF connection between nodes is lost (due to power-loss, environmental obstructions, etc.) critical data can still reach its destination due to the mesh networking capabilities embedded inside the modules. A Sample DigiMesh Network Topology is depicted in Figure 34.

A module within a mesh network is able to determine reliable routes using a routing algorithm and table. The routing algorithm uses a reactive method derived from AODV (Ad-hoc On-demand Distance Vector). An associative routing table is used to map a destination node address with its next hop. By sending a message to the next hop address, either the message will reach its destination or be forwarded to an intermediate node which will route the message on to its destination. A message with a Broadcast address is broadcast to all neighbors. All receiving neighbors will rebroadcast the message and eventually the message will reach all corners of the network. Packet tracking prevents a node from resending a broadcast message twice.

To test the effectiveness of a multi-nodal network, SRD constructed a simple 4-node network in an open air environment. The destination, Node B, was positioned 505 Meters from the base

46

station. This distance is beyond the 372 meters that was determined to be maximum range of the Digi module. Two additional nodes A & C were placed at distances 290 meters and 285 meters from the base station. This creates two possible routes for data being sent to and from node B (sees Figure 35).
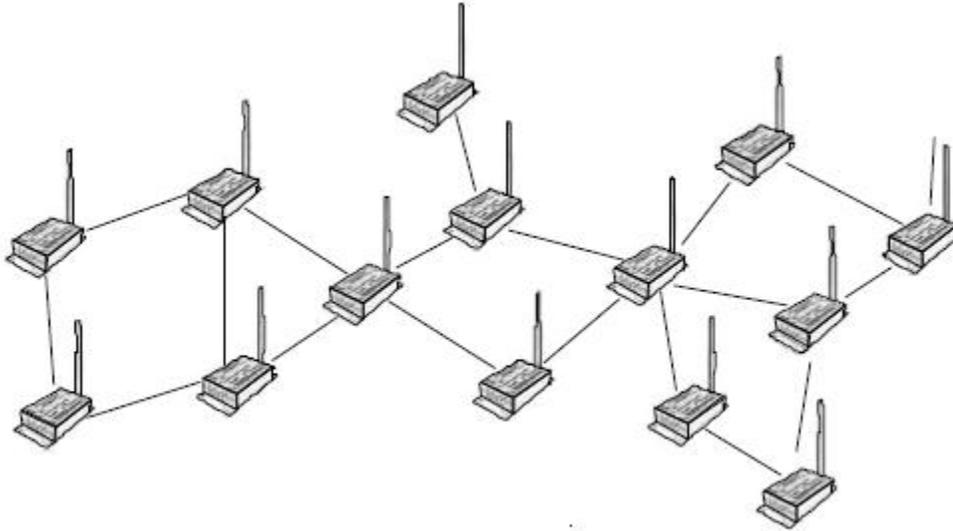

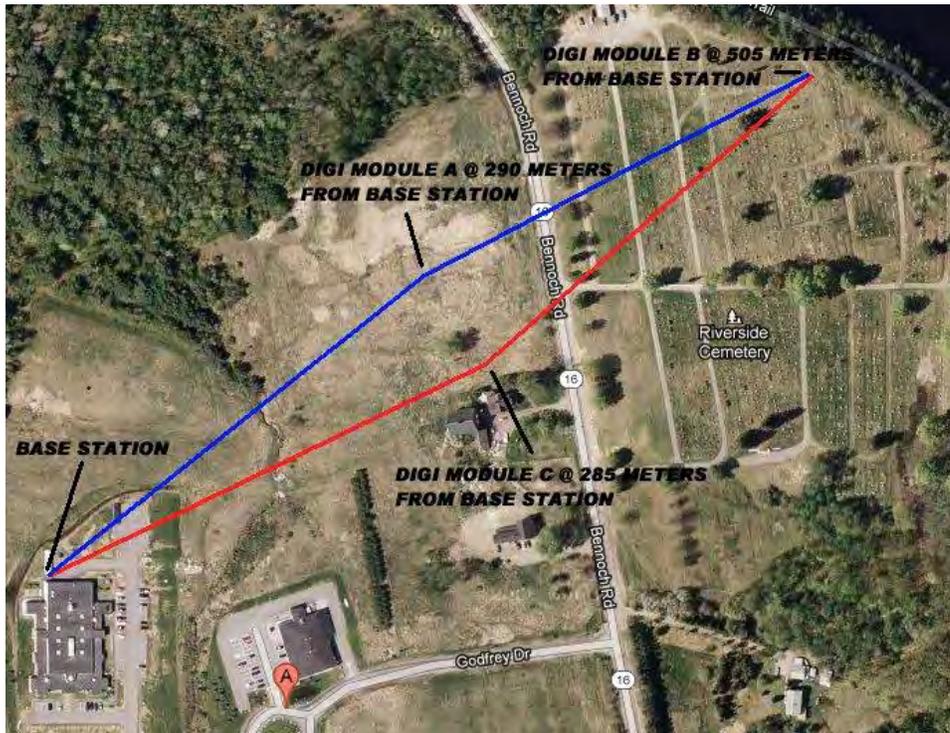**Figure 34: Sample DigiMesh Network.**

Figure 35: Multi-nodal Test Configuration.

From the base station, 1000 packets were sent to Node B. The DigiMesh network determines the most reliable route in which to relay the data, and the number of successful transmissions was recorded for 4 separate cases:

- Both Node A & Node B on
- Node A only
- Node B only
- Both Node A & Node B off

This was done to simulate hardware failure or changes in the node structure, and to determine if the mesh network adapted correctly. As summarized in Figure 36, the 900MHz mesh network was able to successfully route the data through the available nodes to remote module 505 meters away. Communication was able to continue uninterrupted when at least either Node A or Node B was on.
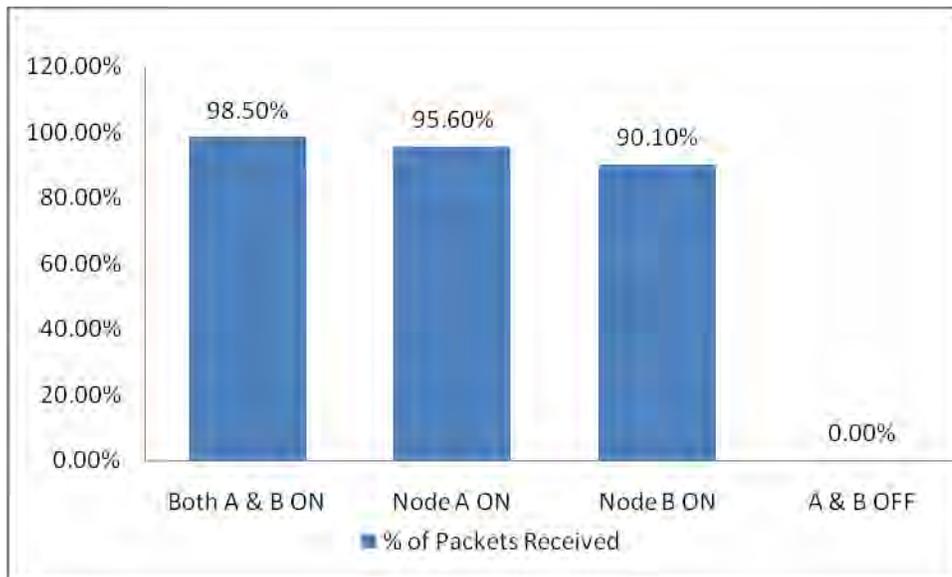
Figure 36: Percentage of successful communication attempts for 4 node conditions in an open field

Real Time Monitoring Considerations

In order to transmit real time atmospheric conditions within a mineshaft, SRD must consider the following factors:

1. Number of sensor nodes,
2. Optimal distance between sensors,
3. Signal Processing hierarchy,
4. Sampling rates and response times, and
5. Temporal accuracy.

Due to the nature of a mesh network, the total number of nodes in the network has an effect on the data rate needed to transfer each node's sensor information back to the base station. Since the number of sensors is not known, nor is the desired area of coverage, it will be necessary to minimize the amount of data transmitted by each node. For this reason, the signal processing must happen on each sensor module individually, rather than at the base station after data collection. In this case, the wireless sensor will only transmit the results of the signal processing

(4 bytes of data per wireless sensor). This would also allow for lower power consumption when lower data rates are sufficient.

The optimal distance between each wireless sensor will depend on the layout of the mine itself. At a transmission power of 10dBm, the 900GHz module can communicate in line-of-site with a module 2230 feet away, according to our test data. This same module in a wooded area, could communicate with a module 380 feet away. This drop in range will be heavily dependent on the environment in the mine, and signal propagation distance will be heavily dependent on mine geometry and the frequency of loss of line-of-sight.

According to the findings of the MSHA report on Underground Communication and Tracking Systems Tests at CONSOL Energy Inc., the Innovative Wireless Technologies AXON Node System, a similar wireless mesh network transceiver operating at 900MHz, was able to transmit up to 1490ft during their track entry test with a transmit power of 10dBm, and 1067 feet through one dip (loss of line-of-sight). We anticipate our module to perform similarly in these conditions, and recommend a maximum distance between nodes of 1000 feet. Using the maximum data rate of 115.2 Kbps for the Digi 900MHz 9Xtend module, a sampling rate of 1 per second, and assuming an average of 10 retransmissions, we could reliably operate 360 sensor nodes all relaying data to a single base station. This would allow maximum transmission coverage of 360,000 feet or 68 miles.

5.1.4.6 Verify operation and performance metrics of sensor array with algorithms

SRD evaluated the performance of the sensor array coupled with the signal processing algorithms to determine the following performance metrics:

1. Detection Times,
2. Probability of False Alarm (PFA),
3. Precision (Response Repeatability), and
4. Accuracy of Quantitation.

Table 17 summarizes the average detection times, using the sensor array "raw" signal responses, for each of the four target gases from testing performed under the gas test protocols previously described Figure 14.   The average detection times are determined by averaging the individual detections times for each of the five replicate trials for each gas at each concentration. Therefore, the average detection times for CH_4, CO, and O_2 are 10-15 seconds from start of exposure, while CO_2 is detected within 30 seconds.

Table 17: Average detection times for target gases.

Gas	Concentration	Hit Detection Time [sec]	Cumulative Average detection time [sec]
Methane (CH$_4$)	0.10%	14	10.5
	0.25%	10	
	0.50%	9	
	1.00%	9	
Carbon monoxide (CO)	10 ppm	17	11.2
	50 ppm	10	
	100 ppm	12	
	600 ppm	8	
	1200 ppm	9	
Oxygen (O$_2$)	20.5%	26	14.6
	21200 ppm	14	
	22%	12	
	19%	10	
	18%	11	
Carbon dioxide (CO$_2$)	0.2%	35	30.4
	0.25%	35	
	0.5%	30	
	0.75%	27	
	1.0%	25	

The performance of the sensor array to correctly identify unknown gases was measured by computing the false alarm rates. Specifically, two alarm types were computed - nuisance alarms (cause due to noise) and false-negatives (missed events).

Table 18 summarizes the performance of the sensors for the rapid exposure of target gases in the presence of standard background conditions.

These results indicate that there are no missed events or NO False Negatives. The total false-alarm rates for CH_4, CO, and O_2 were 0%. The smaller response levels for CO_2 require the use of lower threshold levels in the hit-detection algorithm. Lowering the threshold for hit-detection results in an increase in the number of nuisance false alarms observed at the lower concentrations of 0.2, 0.25 and 0.5%, respectively. This issue will be addressed in Phase II by incorporating a sensor with higher sensitivity toward CO_2.

Table 19 below summarizes the performance of the sensors for the slow varying extended exposure of target gases in the presence of standard background conditions. CO_2 was not tested for the extended concentration ramp testing due to the low sensor response to CO_2. In Phase II, SRD will identify a new sensor that possesses the increased sensitivity to CO_2 needed to reduce the PFA to 0%.

Table 18: False-alarm rates for rapid exposure of target gases.

Gas	Concentration	Nuisance Alarms [%]	Missed Events [%]	Cumulative False-alarm rate [%]
Methane (CH$_4$)	0.10%	0	0	0
	0.25%	0	0	0
	0.50%	0	0	0
	1.00%	0	0	0
Carbon monoxide (CO)	10 ppm	0	0	0
	50 ppm	0	0	0
	100 ppm	0	0	0
	600 ppm	0	0	0
	1200 ppm	0	0	0
Oxygen (O$_2$)	20.5%	0	0	0
	21%	0	0	0
	22%	0	0	0
	19%	0	0	0
	18%	0	0	0
Carbon dioxide (CO$_2$)	0.2%	50	0	50
	0.25%	45	0	45
	0.5%	10	0	10
	0.75%	0	0	0
	1.0%	0	0	0
Average:		5.53	0	5.53

Table 19: False-alarm rates for extended exposure of target gases.

Gas	Duration of exposure [min]	Nuisance Alarms [%]	Missed Events [%]	Cumulative False-alarm rate [%]
Methane (CH$_4$)	30	0	0	0
	50	0	0	0
	210	0	0	0
	410	0	0	0
Carbon monoxide (CO)	30	0	0	0
	50	0	0	0
	210	0	0	0
	410	0	0	0
Oxygen (O$_2$)	30	0	0	0
	50	0	0	0
	210	0	0	0
	410	0	0	0
Average:		0	0	0

In order to evaluate the performance of the sensor in providing real-time concentration estimates, the methane calibration curve was used to provide estimates of concentration for the different methane concentration ramp testing protocols. Figure 37 compares the performance of the estimated concentration, generated using the methane calibration curve, with the ground-truth measurement (i.e. the true concentration of methane gas delivered to the sensor array as a function of time) for the four different concentration ramp rates.
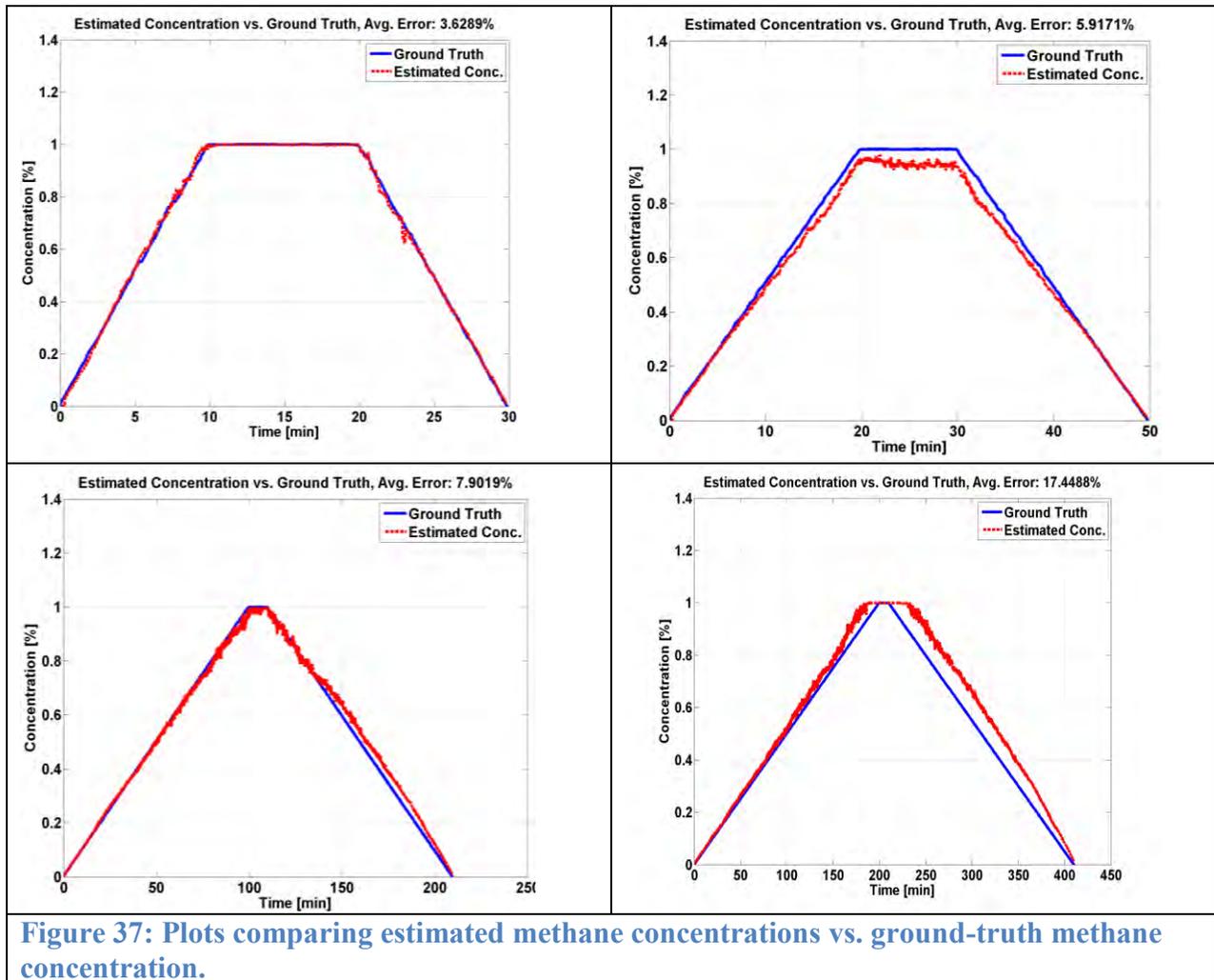

Figure 37: Plots comparing estimated methane concentrations vs. ground-truth methane concentration.

Table 20 summarizes the performance of the methane concentration estimates by reporting the average percentage error over the course of the entire gas exposure for each scenario. The average error in methane concentration estimates all four ramped profile exposure testing conditions was less 9%.

Table 20: Quantitation results for methane under different ramp testing conditions.

Ramp Test Criteria for methane (CH$_4$)	Percentage error in concentration estimates [%]
10 min ramp from 0 to 1%, 10 min at 1%, 10 min ramp down from 1% to 0%	3.63
20 min ramp from 0 to 1%, 10 min at 1%, 20 min ramp down from 1% to 0%	5.92
100 min ramp from 0 to 1%, 10 min at 1%, 100 min ramp down from 1% to 0%	7.90
200 min ramp from 0 to 1%, 10 min at 1%, 200 min ramp down from 1% to 0%	17.45
Average Error:	**8.73**

Figure 38 compares the performance of sensor array with quantitation algorithm for the estimated concentration with the actual CO concentration delivered to the sensor array. Table 21 summarizes the average percentage error from SRD's sensor array and algorithms over the entire gas exposure sequence for each of the four concentration ramp scenarios. The average error in estimates of CO concentration for all the extended exposure testing conditions was less 13%.
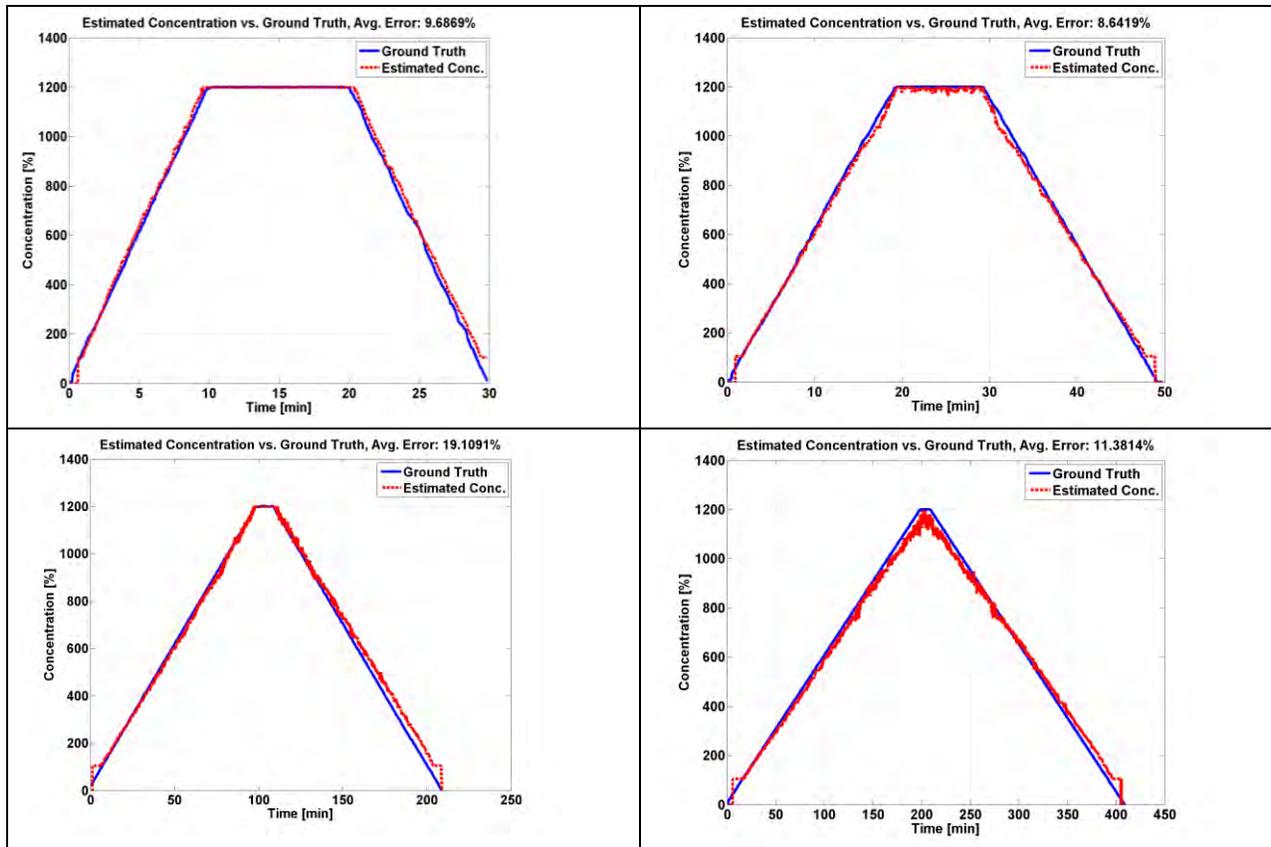
Figure 38: Plots comparing estimated concentrations vs. ground-truth concentration.

Table 21: Quantitation results for CO under different ramp testing conditions.

Ramp Test Criteria for carbonmonoxide (CO)	Percentage error in concentration estimates [%]
10 min ramp from 0 to 1200 ppm, 10 min at 1200 ppm, 10 min ramp down from 1200 ppm to 0%	9.67
20 min ramp from 0 to 1200 ppm, 10 min at 1200 ppm, 20 min ramp down from 1200 ppm to 0%	8.64
100 min ramp from 0 to 1200 ppm, 10 min at 1200 ppm, 100 min ramp down from 1200 ppm to 0%	19.11
200 min ramp from 0 to 1200 ppm, 10 min at 1200 ppm, 200 min ramp down from 1200 ppm to 0%	11.38
Average Error:	**12.20**

Figure 39 compares the estimated concentration, generated using the O_2 calibration curve, with the ground-truth measurement (i.e. the true concentration of O_2 gas that was delivered to the sensor array as a function of time). Table 22 summarizes the average percentage error over the

course of the entire O_2 gas exposure ramps for each of the four scenarios. The average error in O_2 concentration estimates for all the extended exposure testing conditions was less than 3%. It is also important to note that SRD's sensor array and algorithms can detect threshold increases and decreases in O_2 levels indicative of explosive dangers and dangerously low O_2 levels with high accuracy in real-world profiles.
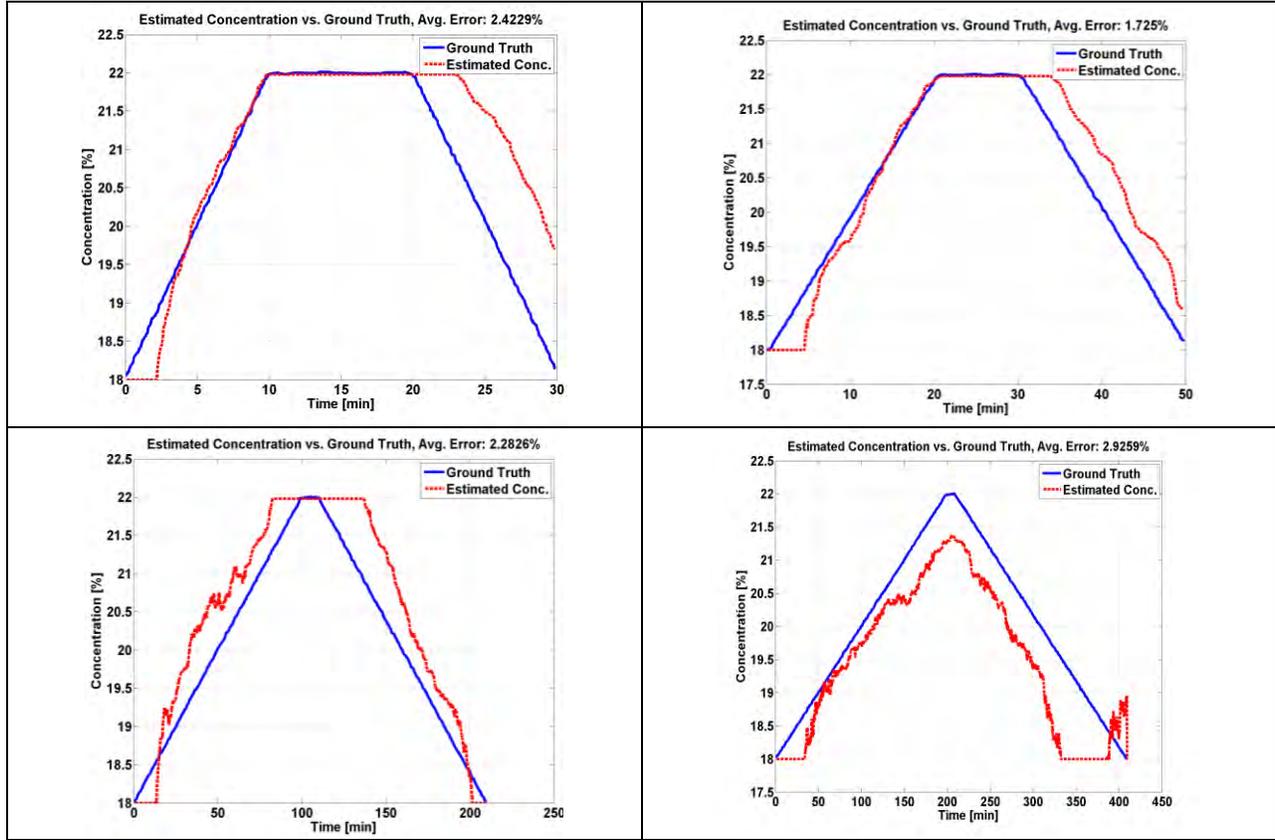

Figure 39: Plots comparing estimated concentrations vs. ground-truth concentration.

Table 22: Quantitation results for O_2 under different ramp testing conditions.

Ramp Test Criteria for Oxygen (O₂)	Percentage error in concentration estimates [%]
10 min ramp from 18% to 22%, 10 min at 22%, 10 min ramp down from 22% to 18%	2.42
20 min ramp from 18% to 22%, 10 min at 22%, 20 min ramp down from 22% to 18%	1.73
100 min ramp from 18% to 22%, 10 min at 22%, 100 min ramp down from 22% to 18%	2.28
200 min ramp from 18% to 22%, 10 min at 22%, 200 min ramp down from 22% to 18%	2.93
Average Error:	**2.34**

Path Loss = 21dBm + 2dB + 2dB - (-110dBm) - 22dBm= 113 dB
(Eq. 2) Link Budget = 18dBm + 2dB

5.1.5 Conclusion

By the completion of this Phase I program, SRD was able to demonstrate the successful design and implementation of a solid-state sensor array, coupled with advanced algorithms, capable of autonomous operation and the real-time, selective detection, identification, and quantification of mining gases including methane (CH_4), carbon monoxide (CO), oxygen (O_2), and carbon dioxide (CO_2) in the presence of typical mining conditions. The Phase I progress and results enabled the three major technical questions for the program to be successfully answered so as to establish a clear foundation from which to build upon in the Phase II follow on effort. Specifically, SRD was able to:

1. Synthesize selectively, sensitive SMO sensors capable of detecting the target gases at the concentration ranges typically present in underground mining operations,
2. Develop algorithms capable of interpreting the "raw" sensor array response signals to detect, identify, and quantify each of the four target gases, and
3. Adapt the sensor array technology to incorporate the necessary filtering and wireless capabilities for robust and networked operation within typical mining environments.

SRD synthesized an array of five (5) chemically tailored SMO sensors that targeted response kinetics with the four mining gases including CH_4, CO, CO_2, and O_2. As the SMO sensor arrays were being synthesized, SRD constructed an automated gas delivery system to deliver the four mine gases at a variety of concentration profiles with specified background conditions. All of the Phase 1 gas testing protocols was performed with the automated gas delivery system. SRD was able to provide ground truth validation of the gas delivery system to support algorithm development in Task 4 and to determine the sensor array's performance metrics in Task 6.

SRD exposed the SMO sensor array to a range of gas testing protocols that fall into the following two scenarios:

1. Detection of sudden change in concentration of each of the mine gases while the concentrations of the other target gases remain constant and
2. Detection of a gradual change in concentration of each target gas while the concentrations of the other target gases in the environment remain constant.

The first scenario (refer back to Figure 14) was designed to simulate the sudden release of a mine gas due to the discovery of a gas pocket, while the second scenario (refer back to Figure 15) was designed to simulate the more difficult and dangerous condition when there is a gradual release of gas from fissures or just from basic consumption during day-to-day mining activities. In order to serve as an early warning device for mines, the concentrations selected for testing of the gases was based on the low, high and critical gas concentrations for each of the target gases (refer back to Table 3).

SRD used the sensor array response data, obtained from all gas testing protocols for both scenarios (sudden change and gradual ramp profiles), to implement a hierarchical algorithm approach to first detect, then identify, and finally quantify the mine gases present in the

environment. In particular, key sensor array response features such as rates of responses and recoveries, response magnitudes, and baseline trends were used for refine the hit detector, train the classifier, and calibrate the quantifier or concentration estimator. The sensor array response data is continuously processed (1 Hz data rate) by the hit-detection algorithm whose function is to monitor if any threats are encountered (i.e. target gases are present). If the algorithm detects an event, it extracts key features of the response and invokes the classification algorithm. The classification algorithm is the second stage of the process. Its main job is to identify an event whenever called into action by the hit-detection algorithm. Once the classification algorithm identifies the gas, it invokes the quantitation algorithm. The quantitation algorithm takes the output of the hit-detection algorithm (key features of response) and classification algorithm (identity of gas), uses this information to provide estimates of the concentration of gas.

SRD established a training database that was used for identification and quantitation of the four mining gases. The database consisted of a library of known sensor response characteristics to the four mine gases at a range of concentration levels. The pattern recognition algorithms query the database in the event a hit (presence of a gas) is determined. SRD uses the information from exposing the selected sensor array to target gases for establishing the databases. The information includes pattern recognition parameters, feature extraction values of sensor response magnitudes, corresponding gas indices, and corresponding gas concentration values. SRD also developed a quantitation algorithm, the third and final stage in the hierarchical algorithm structure. This involved establishing a relationship between the sensors' response magnitudes as a function of gas concentrations, called calibration curves, for CH_4, CO, O_2, and CO_2. The sensor array's "raw" signals were fed into the hierarchical algorithm system to process and interpret the results autonomously, continuously and in real-time (every second).

The performance results obtained from the sensor array, when coupled with the hierarchical algorithms, was determined for all gas testing protocols. These results were used to determine the Phase I sensor array's performance metrics summarized in Table 23. These results outperform the GC/TCD, which requires constant calibration and a highly trained analytical chemist to operate and interpret. SRD's Phase I sensor array and algorithms operates autonomously while providing precise and accurate detection, identification, and quantification of CH_4, CO, O_2, and CO_2, with seconds with no false alarms with the exception of the lower CO_2 concentration levels. Additionally, SRD's Phase I mine detector does NOT require any calibration due to the proven robustness and stability of the SMO sensor array technology and the predicting and adaptive modeling within the hit detection algorithm.

Table 23: Performance metrics for Phase 1 sensor array, coupled with algorithms, toward mining gases.

Performance Metric	CH_4	CO	O_2	CO_2
Ave. Detection Time (sec)	10	11	15	30
Ave. Precision (or RSD)	2.4	2.6	15.6	23.3
Ave. Accuracy (% Error)	8.7	12.2	2.3	Not Tested
False Negative Rate (%)	0	0	0	0
False Positive Rate (%)	0	0	0	5.5
PFA Rate (%)	0	0	0	5.5

SRD also evaluated a Gore water/particulate filter along with an in-house flame arrestor to mitigate the harsh, and potentially explosive, conditions within mining conditions. Specifically, SRD integrated a Gore filter and in-house designed and fabricated flame arrestor into the sensor array sampling system to eliminate particulate matter down to 0.2 microns and to prevent explosions from spreading upstream from the sensor array. The sensors' responses to the four mine gases was measured both with and without the gore filter and flame arrestor inline to prove that the presence of the gore filter and flame arrestor **do not** alter the sensor responses to the four gases.

SRD also evaluated 900 MHz and 2.4 GHz wireless systems to determine which COTS modules would provide the largest transmission range in mining conditions. SRD demonstrated in Task 5 that the 900 MHz Digi 9Xtend module demonstrated superior performance in each of the range testing sections when compared with the AVR 2.4GHz module. Even with a lower transmit power, the 900MHz module had a higher maximum range in all three test conditions: outdoor line-of-sight, inside a metal frames building, and in a wooded area.

SRD constructed a simple 4-node network in an open air environment using the 900MHz Digi Xtend module. This multi-nodal mesh network was evaluated to confirm that strategically placed nodes could effectively extend the wireless transmission range. Therefore, SRD positioned the destination, Node B, 505 Meters from the base station. This distance is beyond the 372 meters that was determined to be maximum range of the Digi module. Two additional nodes A & C were placed at distances 290 meters and 285 meters from the base station. This creates two possible routes for data being sent to and from node B. The 900MHz mesh network was able to successfully route the data through the available nodes to the remote module 505 meters away. Communication was able to continue uninterrupted when at least either Node A or Node B was on. Using the maximum data rate of 115.2 Kbps for the Digi 900MHz 9Xtend module, a sampling rate of 1 Hz, and assuming an average of 10 retransmissions and maximum line-of sight transmission of 1,000 feet, SRD could reliably operate 360 sensor nodes all relaying data to a single base station allowing for transmission coverage of up to 68 miles.

During Phase I, SRD was able to successfully execute all six program tasks:

1. Synthesize and select an SMO sensor array to detect mining gases,
2. Challenge the sensor array to mining gases,
3. Evaluate filters and flame arrestor techniques,

4. Develop sensor array signal processing algorithms,
5. Establish the basis for a wireless sensor network (WSN), and
6. Verify operation and determine performance metrics of sensor array with algorithms.

Therefore, SRD has established, in Phase I, the necessary technical foundation to build a strong Phase II program that will be focused on designing, constructing, verifying, and field-testing prototype mine detectors with expanded capabilities. SRD will incorporate all subsystems including the sensor array, measurement and control electronics, gas-sampling system with integrated inline gore filter and flame arrestor and miniature pump, digital signal processor (DSP) for algorithm processing, power management for battery operation, wireless transmission to enable chemical mapping of the entire mine at central command computer, data storage and download capability, User Interface display, alarm modes, and rugged enclosure. SRD will subject the prototype mine detectors to two field test trials, in an active mine, where the first field trial (~ 2 weeks) will be used to collect critical data to identify any issues within the prototypes that need to be addressed. Any issues identified in the first field test trial will be mitigated prior to the second field test trials (~ 4 weeks). This spiral development will help ensure the prototype mine detectors meet the performance specifications to be defined in the Phase II proposal. The results of the Phase II prototype field testing will govern what the exact Phase III path forward will be.

5.2 Inclusion Enrollment Report

Not applicable – no human subjects were used in this study. An Inclusion Enrollment Report is attached to this submission.

5.3 Publications

No publications were generated from this study.

5.4 Inclusion of Gender and Minority Study Subjects

Not applicable – no human subjects were used in this study.

5.5 Inclusion of Children

Not applicable – no human subjects were used in this study.

5.6 Materials Available for Other Investigators

Other investigators may request research data obtained in this study by contacting the PI listed on the cover page of this report.